

The Kinetic Interpretation of the DGLAP Equation, its Kramers-Moyal Expansion and Positivity of Helicity Distributions

Alessandro Cafarella⁽¹⁾ and Claudio Corianó⁽¹⁾⁽²⁾

⁽¹⁾*Dipartimento di Fisica, Universita' di Lecce
and INFN Sezione di Lecce
Via Arnesano 73100 Lecce, Italy
and*

⁽²⁾*Institute for Fundamental Theory
University of Florida
Gainesville, FL, 32611
alessandro.cafarella@le.infn.it, claudio.coriano@le.infn.it*

Dedicated to Prof. Pierre Ramond for his 60th birthday

Abstract

According to a rederivation - due to Collins and Qiu - the DGLAP equation can be reinterpreted (in leading order) in a probabilistic way. This form of the equation has been used indirectly to prove the bound $|\Delta f(x, Q)| < f(x, Q)$ between polarized and unpolarized distributions, or positivity of the helicity distributions, for any Q . We reanalyze this issue by performing a detailed numerical study of the positivity bounds of the helicity distributions. To obtain the numerical solution we implement an x-space based algorithm for polarized and unpolarized distributions to next-to-leading order in α_s , which we illustrate. We also elaborate on some of the formal properties of the Collins-Qiu form and comment on the underlying regularization, introduce a Kramers-Moyal expansion of the equation and briefly analyze its Fokker-Planck approximation. These follow quite naturally once the master version is given. We illustrate this expansion both for the valence quark distribution q_V and for the transverse spin distribution h_1 .

QCD, the theory of the strong interactions, has reached a stage in which precision measurements of its dynamics have become possible. This scrutiny has allowed to obtain a better understanding of the fundamental structure of the nucleons, disentangling some important features of the underlying quark-gluon interaction with a very good accuracy.

A lot of effort has been undertaken in the last few years to extend the same picture - at the same level of accuracy - also to polarized collisions, with a systematic perturbative analysis performed up to next-to-leading order (NLO) and, in part, in the unpolarized case, also to next-to-next to leading (NNLO) in α_s , the QCD coupling constant.

The aim of this theoretical and experimental effort, in particular at RHIC, the Relativistic Heavy Ion Collider at Brookhaven, is to describe the polarized spin distributions of the nucleon with accuracy.

Therefore the study of possible theoretical constraints on the form of the initial conditions for these distributions and their evolution under the renormalization group (RG) turns out to be very useful.

An interesting constraint relating longitudinally polarized, unpolarized and transversely polarized distributions is Soffer's inequality, which deserves a special attention, since has to be respected by the evolution to any order in α_s . Some tests of the inequality have been performed in the near past, bringing support to it. However, other inequalities are supposed to hold as well.

In this work we perform a NLO analysis of an inequality which relates longitudinally polarized distributions and unpolarized ones. The inequality can be summarized in the statement that helicity distributions (positive and negative) for quarks and gluons have to be positive. The inequality states that

$$|\Delta f(x, Q^2)| < f(x, Q^2) \quad (1)$$

or

$$f^\pm(x, Q^2) > 0 \quad (2)$$

where the \pm refers to the the possible values of the helicities of quarks and gluons. The statement is supposed to hold, at least in leading order, for any Q . To analize the renormalization group evolution of this relation, especially to next-to-leading order, requires some effort since this study involves a combined study of the (longitudinally) polarized and unpolarized evolutions. In this work we present a complete NLO study of the evolution equations starting directly from the helicity basis. Helicities are in fact the basic parton distributions from which other distributions can be built.

Compared to other implementations, in our work we perform a NLO test of the positivity of the helicity distributions using an ansatz due to Rossi [8] which reduces the evolution equations to an infinite set of recursion relations for some scale invariant coefficients. We have developed a complete implementation of this algorithm which will be made available and documented in related work of ours [15].

Various arguments to validate eq. (2) have been presented in the literature. From our perspective, an interesting one has been formulated by Teryaev and Collaborators who have tried to establish a link, to leading order, between evolution equations and their probabilistic interpretation in order to prove Soffer's inequality. Similar arguments hold also in the analysis of eq. (2).

order unpolarized evolution [1] and the arguments of [2] are inspired by the fact that the subtraction terms (the $x = 1$ contributions in the expressions of the kernels, where x is Bjorken's variable), being positive, once they are combined with the bulk ($x < 1$) contributions give a form of the evolution equations which are diagonal in parton type and resemble "kinetic" equations. Our arguments, on this issue, are just a refinement of this previous and influential analysis.

In the recent literature there has been some attention to this feature of the DGLAP evolution, limited to the non-singlet sector, in connection with kinetic theory and the "dynamical renormalization group", in the words of ref. [4].

All the arguments, so far, go back to some important older work of Collins and Qiu who provided an interesting derivation of the (unpolarized) DGLAP equation using Mueller's formalism of cut diagrams. In their paper [1] the authors reinterpreted the DGLAP equation as a kinetic probabilistic equation of Boltzmann type. The authors gave no detail on some of the issues concerning the regularization of their diagrammatic expansion, on which we will elaborate since we need it for our accurate numerical analysis. In our work the Collins-Qiu form of the DGLAP equation is interpreted simply as a *master equation* rather than a Boltzmann equation, given the absence of a 2-to-2 scattering cross section in the probabilistic partonic interpretation. A master equation is governed by transition probabilities and various formal approximations find their way once this conceptual step is made. We illustrate, in the spirit of a stochastic approach to the DGLAP dynamics, how to extract standard differential equations of Kramers-Moyal type for the simplest non-singlet evolutions, those involving valence distributions and transverse spin distributions. Our analysis on this point is self-contained but purposely short, since a more detailed numerical and formal study of this development is under way [15].

We show that the DGLAP dynamics can be described, at least in a formal way, by a differential equation of arbitrarily high order. Truncations of this expansion to the first few orders provide the usual link with the Fokker-Planck approximation, the Langevin equation and its path integral version ¹. The picture one should have in mind, at least in this approximation, is that of a stochastic (brownian) dynamics of Bjorken's variable x in a fictitious time $\log(Q)$, describing the evolution under the renormalization group (RG) whose probability function is the parton distribution itself.

2 Master Equations and Positivity

Let's start considering a generic 1-D master equation for transition probabilities $w(x|x')$ which we interpret as the probability of making a transition to a point x given a starting point x' for a given physical system. The picture we have in mind is that of a gas of particles making collisions in 1-D and entering the interval $(x, x + dx)$ with a probability $w(x|x')$ per single transition, or leaving it with a transition probability $w(x'|x)$. In general one writes down a master equation

$$\frac{\partial}{\partial \tau} f(x, \tau) = \int dx' (w(x|x')f(x', \tau) - w(x'|x)f(x, \tau)) dx'. \quad (3)$$

¹For an example of this interplay between differential and stochastic descriptions we refer the reader to [5]

or a many replicas of walkers of density $j(x, \tau)$ jumping with a pre-assigned probability, according to taste.

The result of Collins a Qiu, who were after a derivation of the DGLAP equation that could include automatically also the “edge point” contributions (or $x=1$ terms of the DGLAP kernels) is in pointing out the existence of a probabilistic picture of the DGLAP dynamics. These edge point terms had been always introduced in the past only by hand and serve to enforce the baryon number sum rule and the momentum sum rule as Q , the momentum scale, varies.

The kinetic interpretation was used in [2] to provide an alternative proof of Soffer’s inequality. We recall that this inequality

$$|h_1(x)| < q^+(x) \quad (4)$$

famous by now, sets a bound on the transverse spin distribution $h_1(x)$ in terms of the components of the positive helicity component of the quarks, for a given flavour. The inequality has to be respected by the evolution. We recall that h_1 , also denoted by the symbol

$$\Delta_T q(x, Q^2) \equiv q^\uparrow(x, Q^2) - q^\downarrow(x, Q^2), \quad (5)$$

has the property of being purely non-singlet and of appearing at leading twist. It is identifiable in transversely polarized hadron-hadron collisions and not in Deep Inelastic Scattering (DIS), where can appear only through an insertion of the electron mass in the unitarity graph of DIS.

The connection between the Collins-Qiu form of the DGLAP equation and the master equation is established as follows. The DGLAP equation, in its original formulation is generically written as

$$\frac{dq(x, Q^2)}{d\log(Q^2)} = \int_x^1 \frac{dy}{y} P(x/y) q(y, Q^2), \quad (6)$$

where we are assuming a scalar form of the equation, such as in the non-singlet sector. The generalization to the singlet sector of the arguments given below is, of course, quite straightforward. To arrive at a probabilistic picture of the equation we start reinterpreting $\tau = \log(Q^2)$ as a time variable, while the parton density $q(x, \tau)$ lives in a one dimensional (Bjorken) x space.

We recall that the kernels are defined as “plus” distributions. Conservation of baryon number, for instance, is enforced by the addition of edge-point contributions proportional to $\delta(1 - x)$.

We start with the following form of the kernel

$$P(z) = \hat{P}(z) - \delta(1 - z) \int_0^1 \hat{P}(z) dz, \quad (7)$$

where we have separated the edge point contributions from the rest of the kernel, here called $\hat{P}(z)$. This manipulation is understood in all the equations that follow. The equation is rewritten in the following form

$$\frac{d}{d\tau} q(x, \tau) = \int_x^1 dy \hat{P}\left(\frac{x}{y}\right) \frac{q(y, \tau)}{y} - \int_0^x dy \hat{P}\left(\frac{y}{x}\right) \frac{q(x, \tau)}{x} \quad (8)$$

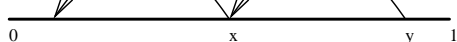


Figure 1: The constrained random walk of the parton densities

Now, if we define

$$w(x|y) = \frac{\alpha_s}{2\pi} \hat{P}(x/y) \frac{\theta(y > x)}{y} \quad (9)$$

(8) becomes a master equation for the probability function $q(x, \tau)$

$$\frac{\partial}{\partial \tau} q(x, \tau) = \int dx' (w(x|x')q(x', \tau) - w(x'|x)q(x, \tau)) dx'. \quad (10)$$

There are some interesting features of this special master equation. Differently from other master equations, where transitions are allowed from a given x both toward $y > x$ and $y < x$, in this case, transitions toward x take place only from values $y > x$ and leave the momentum cell $(x, x + dx)$ only toward smaller y values (see Fig.(1)).

Clearly, this sets a direction of the kinetic evolution of the densities from large x values toward smaller- x values as τ , the fictitious “time” variable, increases.

Probably this is the simplest illustration of the fact that parton densities, at large final evolution scales, are dominated by their small- x behaviour. As the “randomly moving partons” reach the $x \approx 0$ region of momentum space, they find no space where to go, while other partons tend to pile up toward the same region from above. This is the picture of a random walk biased to move downward (toward the small- x region) and is illustrated in Fig. (1).

3 Probabilistic Kernels

We briefly discuss some salient features of the structure of the kernels in this approach and comment on the type of regularization involved in order to define them appropriately.

We recall that unpolarized and polarized kernels, in leading order, are given by

$$\begin{aligned} P_{NS}^{(0)} &= P_{qq}^{(0)} = C_F \left(\frac{2}{(1-x)_+} - 1 - x + \frac{3}{2} \delta(1-x) \right) \\ P_{qg}^{(0)} &= 2T_f (x^2 + (1-x)^2) \\ P_{gq}^{(0)} &= C_F \frac{1 + (1-x)^2}{x} \\ P_{gg}^{(0)} &= 2N_c \left(\frac{1}{(1-x)_+} + \frac{1}{x} - 2 + x(1-x) \right) + \frac{\beta_0}{2} \delta(1-x) \end{aligned} \quad (11)$$

where

$$C_F = \frac{N_C^2 - 1}{2N_C}, \quad T_f = T_R n_f = \frac{1}{2} n_f, \quad \beta_0 = \frac{11}{3} N_C - \frac{4}{3} T_f \quad (12)$$

and

$$\Delta P_{NS}^{(0)} = \Delta P_{qq}^{(0)}$$

$$\begin{aligned}
\Delta P_{qq}^{(0)} &= 2T_f(2x-1) \\
\Delta P_{gq}^{(0)} &= C_F(2-x) \\
\Delta P_{gg}^{(0)} &= 2N_c \left(\frac{1}{(1-x)_+} - 2x + 1 \right) + \delta(1-x) \frac{\beta_0}{2},
\end{aligned} \tag{13}$$

while the LO transverse kernels are given by

$$\Delta_T P_{qq}^{(0)} = C_F \left(\frac{2}{(1-x)_+} - 2 + \frac{3}{2} \delta(1-x) \right). \tag{14}$$

The unpolarized kernels should be compared with the Collins-Qiu form

$$\begin{aligned}
P_{qq} &= \gamma_{qq} - \delta(1-x) \int_0^1 dz \gamma_{qq} \\
P_{gg} &= \gamma_{gg} - \left(n_f \int_0^1 dz \gamma_{qg} + \frac{1}{2} \int_0^1 dz \gamma_{gg} \right) \delta(1-x) \\
P_{qg} &= \gamma_{qg} \\
P_{gq} &= \gamma_{gq}
\end{aligned} \tag{15}$$

where

$$\begin{aligned}
\gamma_{qq} &= C_F \left(\frac{2}{1-x} - 1 - x \right) \\
\gamma_{qg} &= (2x-1) \\
\gamma_{gg} &= C_F(2-x) \\
\gamma_{gg} &= 2N_c \left(\frac{1}{1-x} + \frac{1}{x} - 2 + x(1-x) \right).
\end{aligned} \tag{16}$$

These kernels need a suitable regularization to be well defined. Below we will analize the implicit regularization underlying eq. (15). One observation is however almost immediate: the component P_{gg} is not of the form given by eq. (7). In general, therefore, in the singlet case, the generalization of eq. (7) is given by

$$P(x) = \hat{P}_1(x) - \delta(1-x) \int_0^1 \hat{P}_2(z) dz \tag{17}$$

and a probabilistic interpretation is more complex compared to the non-singlet case and has been discussed in the original literature [1].

4 Convolutions and Master Form of the Singlet

Distributions are folded with the kernels and the result rearranged in order to simplify the structure of the equations. Since in the previous literature this is done in a rather involved way [6] we provide here a simplificaton, from which the equivalence of the various

is the simple relation

$$\int_x^1 \frac{dy}{y(1-y)_+} f(x/y) = \int_x^1 \frac{dy}{y} \frac{yf(y) - xf(x)}{y-x} - \log(1-x)f(x) \quad (18)$$

in which, on the right hand side, regularity of both the first and the second term is explicit. For instance, the evolution equations become

$$\begin{aligned} \frac{dq}{d \log(Q^2)} &= 2C_F \int \frac{dy}{y} \frac{yq(y) - xq(x)}{y-x} + 2C_F \log(1-x) q(x) - \int_x^1 \frac{dy}{y} (1+z) q(y) + \frac{3}{2} C_F q(x) \\ &\quad + n_f \int_x^1 \frac{dy}{y} (z^2 + (1-z)^2) g(y) \\ \frac{dg}{d \log(Q^2)} &= C_F \int_x^1 \frac{dy}{y} \frac{1 + (1-z)^2}{z} q(y) + 2N_c \int_x^1 \frac{dy}{y} \frac{yf(y) - xf(x)}{y-x} g(y) \\ &\quad + 2N_c \log(1-x) g(x) + 2N_c \int_x^1 \frac{dy}{y} \left(\frac{1}{z} - 2 + z(1-z) \right) g(y) + \frac{\beta_0}{2} g(x) \end{aligned} \quad (19)$$

with $z \equiv x/y$. The same simplified form is obtained from the probabilistic version, having defined a suitable regularization of the edge point singularities in the integrals over the components $\gamma_{ff'}$ in eq. (16). The canonical expressions of the kernels (21), expressed in terms of “+” distributions, can also be rearranged to look like their equivalent probabilistic form by isolating the edge-point contributions hidden in their “+” distributions. We get the expressions

$$\begin{aligned} P_{qq \ NS}^{(0)} &= P_{qq}^{(0)} = C_F \left(\frac{2}{(1-x)} - 1 - x \right) - \left(C_F \int_0^1 \frac{dz}{1-z} - \frac{3}{2} \right) \delta(1-x) \\ P_{gg}^{(0)} &= 2N_c \left(\frac{1}{(1-x)} + \frac{1}{x} - 2 + x(1-x) \right) - \left(2N_c \int_0^1 \frac{dz}{1-z} - \frac{\beta_0}{2} \right) \delta(1-x) \end{aligned} \quad (20)$$

and

$$\begin{aligned} \Delta P_{qq}^{(0)} &= C_F \left(\frac{2}{(1-x)} - 1 - x \right) - C_F \left(\int_0^1 \frac{dz}{1-z} - \frac{3}{2} \right) \delta(1-x) \\ \Delta P_{gg}^{(0)} &= 2N_c \left(\frac{1}{1-x} - 2x + 1 \right) - \left(2N_c \int_0^1 \frac{dz}{1-z} - \frac{\beta_0}{2} \right) \delta(1-x), \end{aligned} \quad (21)$$

the other expressions remaining invariant. In appendix A we provide some technical details on the equivalence between the convolutions obtained using these kernels with the standard ones.

A master form of the singlet (unpolarized) equation is obtained by a straightforward change of variable in the decreasing terms. We obtain

$$\begin{aligned} \frac{dq}{d\tau} &= \int_x^{1-\Lambda} \frac{dy}{y} \gamma_{qq}(x/y) q(y) - \int_0^{x-\Lambda} \frac{dy}{y} \gamma_{qq}(y/x) q(x) \\ \frac{dg}{d\tau} &= \int_x^{1-\Lambda} \frac{dy}{y} \gamma_{gg}(x/y) - n_f \int_0^x \gamma_{qg}(y/x) g(x) \\ &\quad - \frac{1}{2} \int_{\Lambda}^{x-\Lambda} \gamma_{gg}(y/x) g(x) + \int_x^1 \frac{dy}{y} \gamma_{qg}(x/y) q(y) \end{aligned} \quad (22)$$

or this aspect is left in appendix B. The (regulated) transition probabilities are then given by

$$\begin{aligned}
w_{qq}(x|y) &= \gamma_{qq}(x/y) \frac{\theta(y > x)\theta(y < 1 - \Lambda)}{y} \\
w_{qq}(y|x) &= \gamma_{qq}(y/x) \frac{\theta(y < x - \Lambda)\theta(y > 0)}{x} \\
w_{gg}(x|y) &= \gamma_{gg}(x/y) \frac{\theta(y > x)\theta(y < 1 - \Lambda)}{y} \\
w_{qq}(y|x) &= \left(n_f \gamma_{qq}(y/x) - \frac{1}{2} \gamma_{gg}(y/x) \right) \frac{\theta(y < x - \Lambda)\theta(y > 0)}{x} \\
w_{gq}(y|x) &= \gamma_{gq}(x/y) \frac{\theta(y > x)\theta(y < 1 - \Lambda)}{y} \\
w_{gq}(x|y) &= 0,
\end{aligned} \tag{23}$$

as one can easily deduct from the form of eq. (10).

5 A Kramers-Moyal Expansion for the DGLAP Equation

Kramers-Moyal (KM) expansions of the master equations (backward or forward) are sometimes useful in order to gain insight into the master equation itself, since they may provide a complementary view of the underlying dynamics.

The expansion allows to get rid of the integral which characterizes the master equation, at the cost of introducing a differential operator of arbitrary order. For the approximation to be useful, one has to stop the expansion after the first few orders. In many cases this turns out to be possible. Examples of processes of this type are special Langevin processes and processes described by a Fokker-Planck operator. In these cases the probabilistic interpretation allows us to write down a fictitious lagrangean, a corresponding path integral and solve for the propagators using the Feynman-Kac formula. For definiteness we take the integral to cover all the real axis in the variable x'

$$\frac{\partial}{\partial \tau} q(x, \tau) = \int_{-\infty}^{\infty} dx' (w(x|x')q(x', \tau) - w(x'|x)q(x, \tau)) dx'. \tag{24}$$

As we will see below, in the DGLAP case some modifications to the usual form of the KM expansion will appear. At this point we perform a KM expansion of the equation in the usual way. We make the substitutions in the master equation $y \rightarrow x - y$ in the first term and $y \rightarrow x + y$ in the second term

$$\frac{\partial}{\partial \tau} q(x, \tau) = \int_{-\infty}^{\infty} dy (w(x|x-y)q(x-y, \tau) - w(x-y|x)q(x, \tau)), \tag{25}$$

identically equal to

$$\frac{\partial}{\partial \tau} q(x, \tau) = \int_{-\infty}^{\infty} dy (w(x+y-y'|x-y')q(x-y', \tau) - w(x+y'|x)q(x, \tau)), \tag{26}$$

can be related using a Taylor (or KM) expansion of the first term

$$\frac{\partial}{\partial \tau} q(x, \tau) = \int_{-\infty}^{\infty} dy \sum_{n=1}^{\infty} \frac{(-y)^n}{n!} \frac{\partial^n}{\partial x^n} (w(x+y|x)q(x, \tau)) \quad (27)$$

where the $n = 0$ term has canceled between the first and the second contribution coming from (26). The result can be written in the form

$$\frac{\partial}{\partial \tau} q(x, \tau) = \sum_{n=1}^{\infty} \frac{(-y)^n}{n!} \frac{\partial^n}{\partial x^n} (a_n(x)q(x, \tau)) \quad (28)$$

where

$$a_n(x) = \int_{-\infty}^{\infty} dy (y-x)^n w(y|x). \quad (29)$$

In the DGLAP case we need to amend the former derivation, due to the presence of boundaries ($0 < x < 1$) in the Bjorken variable x . For simplicity we will focus on the non-singlet case. We rewrite the master equation using the same change of variables used above

$$\begin{aligned} \frac{\partial}{\partial \tau} q(x, \tau) = & \int_x^1 dy w(x|y)q(y, \tau) - \int_0^x dy w(y|x)q(x, \tau) \\ & - \int_0^{\alpha(x)} dy w(x+y|x) * q(x, \tau) + \int_0^{-x} dy w(x+y|x)q(x, \tau), \end{aligned} \quad (30)$$

where we have introduced the simplest form of the Moyal product ²

$$w(x+y|x) * q(x) \equiv w(x+y|x) e^{-y \left(\overleftarrow{\partial}_x + \overrightarrow{\partial}_x \right)} q(x, \tau) \quad (31)$$

and $\alpha(x) = x - 1$. The expansion is of the form

$$\frac{\partial}{\partial \tau} q(x, \tau) = \int_{\alpha(x)}^{-x} dy w(x+y|x)q(x, \tau) - \sum_{n=1}^{\infty} \int_0^{\alpha(x)} dy \frac{(-y)^n}{n!} \partial_x^n (w(x+y|x)q(x, \tau)) \quad (32)$$

which can be reduced to a differential equation of arbitrary order using simple manipulations. We recall that the Fokker-Planck approximation is obtained stopping the expansion at the second order

$$\frac{\partial}{\partial \tau} q(x, \tau) = a_0(x) - \partial_x (a_1(x)q(x)) + \frac{1}{2} \partial_x^2 (a_2(x)q(x, \tau)) \quad (33)$$

with

$$a_n(x) = \int dy y^n w(x+y, x) \quad (34)$$

being moments of the transition probability function w . Given the boundary conditions on the Bjorken variable x , even in the Fokker-Planck approximation, the Fokker-Planck version of the DGLAP equation is slightly more involved than Eq. (33) and the coefficients $a_n(x)$ need to be redefined.

²A note for noncommutative geometers: this simplified form is obtained for a dissipative dynamics when the \mathbf{p} 's of phase space are replaced by constants. Here we have only one variable: x

The probabilistic interpretation of the DGLAP equation motivates us to investigate the role of the Fokker-Planck (FP) approximation to the equation and its possible practical use. We should start by saying a word of caution regarding this expansion.

In the context of a random walk, an all-order derivative expansion of the master equation can be arrested to the first few terms either if the conditions of Pawula's theorem are satisfied -in which case the FP approximation turns out to be exact- or if the transition probabilities show an exponential decay above a certain distance allowed to the random walk. Since the DGLAP kernels show only an algebraic decay in x , and there isn't any explicit scale in the kernel themselves, the expansion is questionable. However, from a formal viewpoint, it is still allowed. With these caveats in mind we proceed to investigate the features of this expansion.

We redefine

$$\begin{aligned}\tilde{a}_0(x) &= \int_{\alpha(x)}^{-x} dy w(x+y|x) q(x, \tau) \\ a_n(x) &= \int_0^{\alpha(x)} dy y^n w(x+y|x) q(x, \tau) \\ \tilde{a}_n(x) &= \int_0^{\alpha(x)} dy y^n \partial_x^n (w(x+y|x) q(x, \tau)) \quad n = 1, 2, \dots\end{aligned}\tag{35}$$

For the first two terms ($n = 1, 2$) one can easily work out the relations

$$\begin{aligned}\tilde{a}_1(x) &= \partial_x a_1(x) - \alpha(x) \partial_x \alpha(x) w(x + \alpha(x)|x) q(x, \tau) \\ \tilde{a}_2(x) &= \partial_x^2 a_2(x) - 2\alpha(x) (\partial_x \alpha(x))^2 w(x + \alpha(x)|x) q(x, \tau) - \alpha(x)^2 \partial_x \alpha(x) \partial_x (w(x + \alpha(x)|x) q(x, \tau)) \\ &\quad - \alpha^2(x) \partial_x \alpha(x) \partial_x (w(x + y|x) q(x, \tau))|_{y=\alpha(x)}\end{aligned}\tag{36}$$

Let's see what happens when we arrest the expansion (32) to the first 3 terms. The Fokker-Planck version of the equation is obtained by including in the approximation only \tilde{a}_n with $n = 0, 1, 2$.

The Fokker-Planck limit of the (non-singlet) equation is then given by

$$\frac{\partial}{\partial \tau} q(x, \tau) = \tilde{a}_0(x) + \tilde{a}_1(x) - \frac{1}{2} \tilde{a}_2(x)\tag{37}$$

which we rewrite explicitly as

$$\begin{aligned}\frac{\partial}{\partial \tau} q(x, \tau) &= C_F \left(\frac{85}{12} + \frac{3}{4x^4} - \frac{13}{3x^3} + \frac{10}{x^2} - \frac{12}{x} + 2 \log \left(\frac{1-x}{x} \right) \right) q(x) \\ &\quad + C_F \left(9 - \frac{1}{2x^3} + \frac{3}{x^2} - \frac{7}{x} - \frac{9}{2} \right) \partial_x q(x, \tau) \\ &\quad + C_F \left(\frac{9}{4} + \frac{1}{8x^2} - \frac{5}{6x} - \frac{5x}{2} + \frac{23x^2}{24} \right) \partial_x^2 q(x, \tau).\end{aligned}\tag{38}$$

A similar approach can be followed also for other cases, for which a probabilistic picture (a derivation of Collins-Qiu type) has not been established yet, such as for h_1 . We describe briefly how to proceed in this case.

form. This is possible since the subtraction terms can be written as integrals of a positive function. A possibility is to choose the transition probabilities

$$\begin{aligned} w_1[x|y] &= \frac{C_F}{y} \left(\frac{2}{1-x/y} - 2 \right) \theta(y > x) \theta(y < 1) \\ w_2[y|x] &= \frac{C_F}{x} \left(\frac{2}{1-y/x} - \frac{3}{2} \right) \theta(y > -x) \theta(y < 0) \end{aligned} \quad (39)$$

which reproduce the evolution equation for h_1 in master form

$$\frac{dh_1}{d\tau} = \int_0^1 dy w_1(x|y) h_1(y, \tau) - \int_0^1 dy w_2(y|x) h_1(x, \tau). \quad (40)$$

The Kramers-Moyal expansion is derived as before, with some slight modifications. The result is obtained introducing an intermediate cutoff which is removed at the end. In this case we get

$$\begin{aligned} \frac{dh_1}{d\tau} &= C_F \left(\frac{17}{3} - \frac{2}{3x^3} + \frac{3}{x^2} - \frac{6}{x} + 2 \log \left(\frac{1-x}{x} \right) \right) h_1(x, \tau) \\ &\quad + C_F \left(6 + \frac{2}{3x^2} - \frac{3}{x} - \frac{11x}{3} \right) \partial_x h_1(x, \tau) \\ &\quad + C_F \left(\frac{3}{2} - \frac{1}{3x} - 2x + \frac{5x^2}{6} \right) \partial_x^2 h_1(x, \tau). \end{aligned}$$

Notice that compared to the standard Fokker-Planck approximation, the boundary now generates a term on the left-hand-side of the equation proportional to $q(x)$ which is absent in eq. (33). This and higher order approximations to the DGLAP equation can be studied systematically both analytically and numerically and it is possible to assess the validity of the approximation [15].

7 Helicities to LO

As we have mentioned above, an interesting version of the usual DGLAP equation involves the helicity distributions.

We start introducing [2] the DGLAP kernels for fixed helicites $P_{++}(z) = (P(z) + \Delta P(z))/2$ and $P_{+-}(z) = (P(z) - \Delta P(z))/2$ which will be used below. $P(z)$ denotes (generically) the unpolarized kernels, while the $\Delta P(z)$ are the longitudinally polarized ones. These definitions, throughout the paper, are meant to be expanded up to NLO, the order at which our numerical analysis holds.

The equations, in the helicity basis, are

$$\begin{aligned} \frac{dq_+(x)}{dt} &= \frac{\alpha_s}{2\pi} \left(P_{++}^{qq} \left(\frac{x}{y} \right) \otimes q_+(y) + P_{+-}^{qq} \left(\frac{x}{y} \right) \otimes q_-(y) \right. \\ &\quad \left. + P_{++}^{qg} \left(\frac{x}{y} \right) \otimes g_+(y) + P_{+-}^{qg} \left(\frac{x}{y} \right) \otimes g_-(y) \right), \\ \frac{dq_-(x)}{dt} &= \frac{\alpha_s}{2\pi} \left(P_{+-} \left(\frac{x}{y} \right) \otimes q_+(y) + P_{++} \left(\frac{x}{y} \right) \otimes q_-(y) \right) \end{aligned}$$

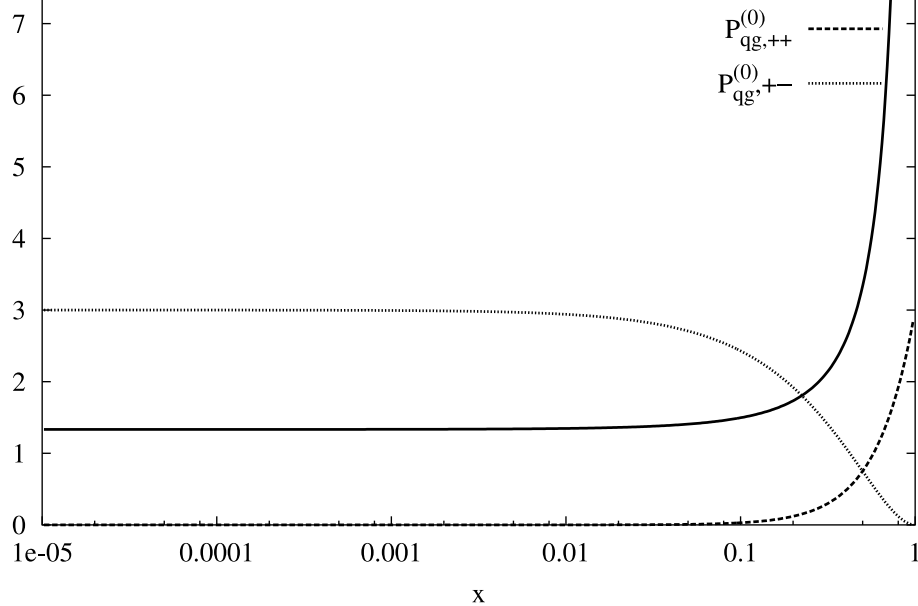


Figure 2: LO kernels (qq and qg) in the helicity basis.

$$\begin{aligned}
& + P_{+-}^{gg} \left(\frac{x}{y} \right) \otimes g_+(y) + P_{++}^{gg} \left(\frac{x}{y} \right) \otimes g_-(y)), \\
\frac{dg_+(x)}{dt} &= \frac{\alpha_s}{2\pi} (P_{++}^{gg} \left(\frac{x}{y} \right) \otimes q_+(y) + P_{+-}^{gg} \left(\frac{x}{y} \right) \otimes q_-(y) \\
& + P_{+-}^{gg} \left(\frac{x}{y} \right) \otimes g_+(y) + P_{++}^{gg} \left(\frac{x}{y} \right) \otimes g_-(y)), \\
\frac{dg_-(x)}{dt} &= \frac{\alpha_s}{2\pi} (P_{+-}^{gg} \left(\frac{x}{y} \right) \otimes q_+(y) + P_{++}^{gg} \left(\frac{x}{y} \right) \otimes q_-(y) \\
& + P_{+-}^{gg} \left(\frac{x}{y} \right) \otimes g_+(y) + P_{++}^{gg} \left(\frac{x}{y} \right) \otimes g_-(y)). \tag{41}
\end{aligned}$$

The non-singlet (valence) analogue of this equation is also easy to write down

$$\begin{aligned}
\frac{dq_{+,V}(x)}{dt} &= \frac{\alpha_s}{2\pi} (P_{++} \left(\frac{x}{y} \right) \otimes q_{+,V}(y) + P_{+-} \left(\frac{x}{y} \right) \otimes q_{-,V}(y)), \\
\frac{dq_{-,V}(x)}{dt} &= \frac{\alpha_s}{2\pi} (P_{+-} \left(\frac{x}{y} \right) \otimes q_{+,V}(y) + P_{++} \left(\frac{x}{y} \right) \otimes q_{-,V}(y)). \tag{42}
\end{aligned}$$

where the $q_{\pm,V} = q_{\pm} - \bar{q}_{\pm}$ are the valence components of fixed helicites. The kernels in this basis are given by

$$\begin{aligned}
P_{NS\pm,++}^{(0)} &= P_{qq,++}^{(0)} = P_{qq}^{(0)} \\
P_{qq,+-}^{(0)} &= P_{qq,-+}^{(0)} = 0 \\
P_{qg,++}^{(0)} &= n_f x^2 \\
P_{qg,+-} &= P_{qg,-+} = n_f (x-1)^2 \\
P_{gq,++} &= P_{gq,--} = C_F \frac{1}{x} \\
P_{gg,++}^{(0)} &= P_{gg,++}^{(0)} = N_c \left(\frac{2}{(1-x)_+} + \frac{1}{x} - 1 - x - x^2 \right) + \beta_0 \delta(1-x)
\end{aligned}$$

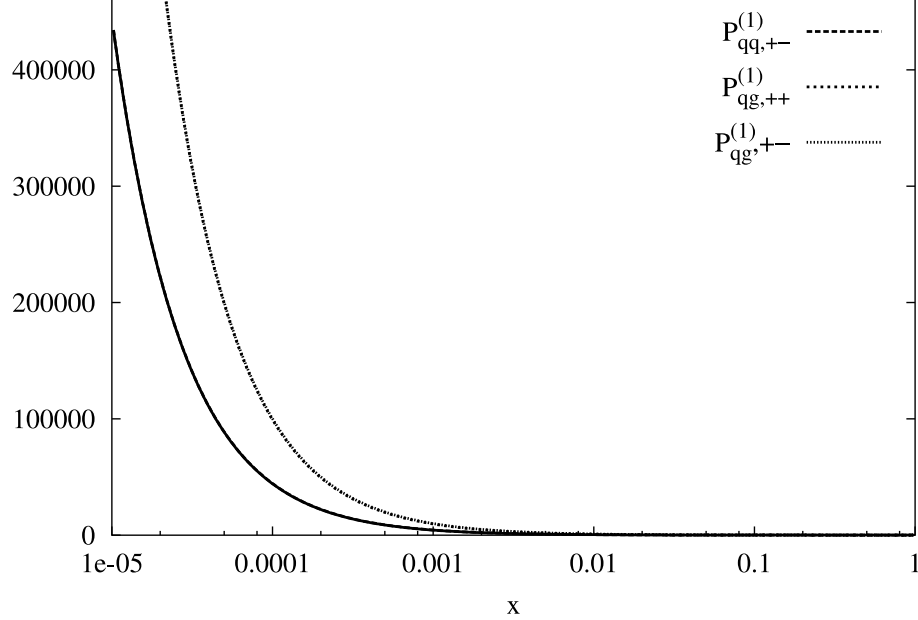


Figure 3: NLO kernels (qq and qg) in the helicity basis.

$$P_{gg,+-}^{(0)} = N_c \left(3x + \frac{1}{x} - 3 - x^2 \right) \quad (43)$$

Taking linear combinations of these equations (adding and subtracting), one recovers the usual evolutions for unpolarized $q(x)$ and longitudinally polarized $\Delta q(x)$ distributions. We recall that the unpolarized distributions, the polarized and the transversely polarized $q_T(x)$ are related by

$$\begin{aligned} q(x) &= q_+(x) + q_-(x) = q_{+T}(x) + q_{-T}(x) \\ \Delta q(x) &= q_+(x) - q_-(x) \end{aligned} \quad (44)$$

at any Q of the evolution and, in particular, at the boundary of the evolution.

Similar definition have been introduced for the gluon sector with $G_{\pm}(x)$ denoting the fixed helicities of the gluon distributions with $\Delta g(x) = g_+(x) - g_-(x)$ and $g(x) = g_+(x) + g_-(x)$ being the corresponding longitudinal asymmetry and the unpolarized density respectively.

8 Summary of Positivity Arguments

Let's recapitulate here the basic arguments [2] that are brought forward in order to prove the positivity of the evolution to NLO.

If

$$|\Delta P(z)| \leq P(z), z < 1 \quad (45)$$

then both kernels $P_{++}(z)$ and $P_{+-}(z)$ are positive as far as $z < 1$.

The singular contributions at $z = 1$, which appear as subtraction terms in the evolution and which could, in principle, alter positivity, appear only in diagonal form, which means that they are only contained in P_{++} , multiplied by the single functions $q_+(x)$ or $q_-(x)$

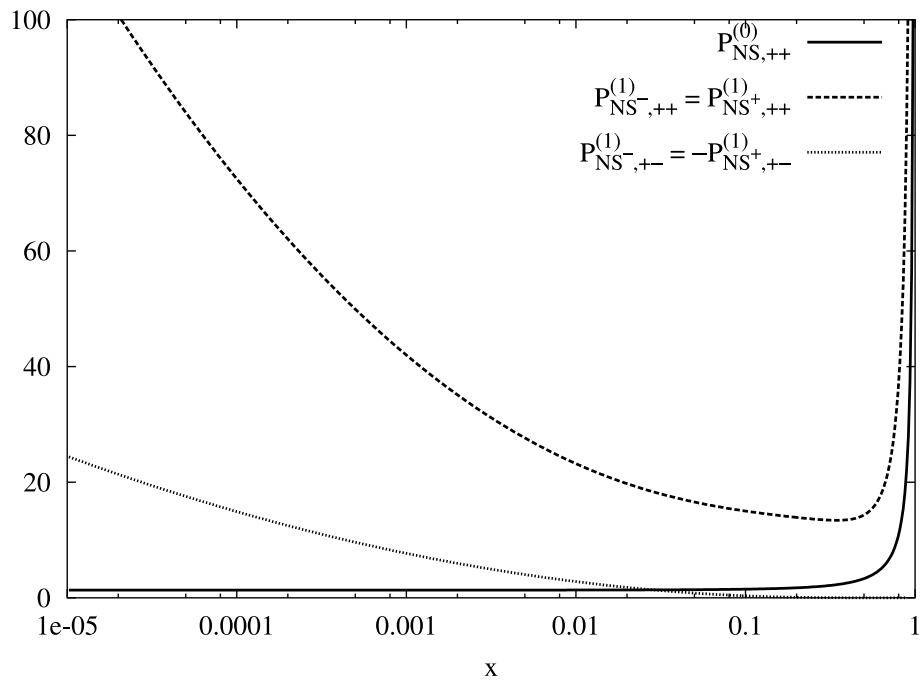


Figure 4: Nonsinglet kernels in the helicity basis.

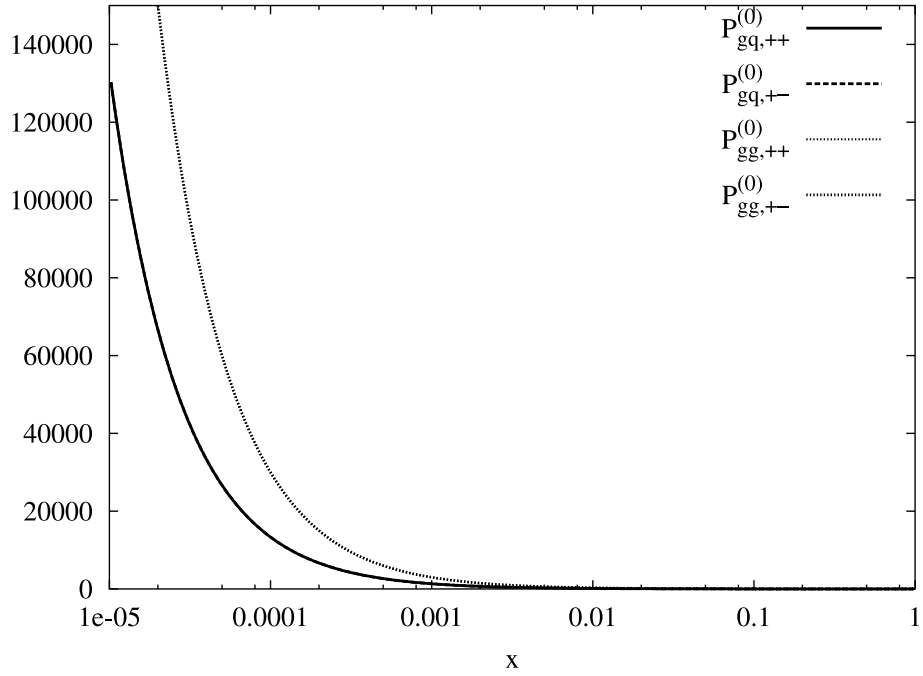


Figure 5: LO kernels (gq and gg) in the helicity basis.

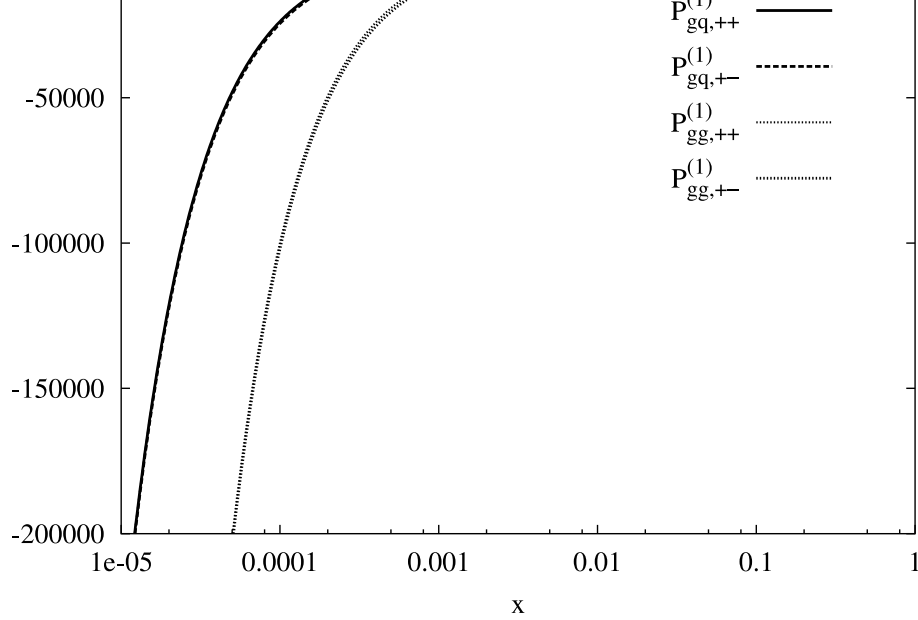


Figure 6: NLO kernels (gq and gg) in the helicity basis.

$$\frac{dq_+(x)}{dt} = \frac{\alpha_s}{2\pi} P_{++}^{qq} \left(\frac{x}{y} \right) \otimes q_+(y) + \dots \quad (46)$$

$$\frac{dq_-(x)}{dt} = \frac{\alpha_s}{2\pi} P_{++}^{qq} \left(\frac{x}{y} \right) \otimes q_+(y) + \dots \quad (47)$$

$$\frac{dg_+(x)}{dt} = \frac{\alpha_s}{2\pi} P_{++}^{gg} \left(\frac{x}{y} \right) \otimes g_+(y) + \dots \quad (48)$$

Let's focus just on the equation for q_+ (46). Rewriting the diagonal contribution as a master equation

$$\frac{dq_+(x)}{dt} = \int dx' (w_{++}(x|x') q_+(x', \tau) - w_{++}(x'|x) q_+(x, \tau)) dx' + \dots \quad (49)$$

in terms of a transition probability

$$w_{++}(x|y) = \frac{\alpha_s}{2\pi} \hat{P}_{++}(x/y) \theta(y > x) \quad (50)$$

which can be easily established to be positive, as we are going to show rigorously below, as far as all the remaining terms (the ellipses) are positive. We have performed a detailed numerical analysis to show the positivity of the contributions at $x = 1$.

This last condition is also clearly satisfied, since the $\delta(1 - z)$ contributions appear only in P_{++} and are diagonal in the helicity of the various flavours (q, g). For a rigorous proof of the positivity of the solutions of master equations we proceed as follows.

Let $q(x, \tau)$ be a positive distribution for $\tau < \tau_c$ and let us assume that it vanishes at $\tau = \tau_c$, after which it turns negative. We also assume that the evolution of $q(x, \tau)$ is of the form (7) with positive transition probabilities $w(x|y)$ and $w(y|x)$. Notice that since the function is continuous together with its first derivative and decreasing, continuity of

requires that at $\tau = \tau_c$

$$\frac{dq(x)}{dt} = \int dx' w(x|x') q(x', \tau) \quad (51)$$

which is positive, and we have a contradiction. We can picture the evolution in τ of these functions as a family of curves getting support to smaller and smaller x-values as τ grows and being almost vanishing at intermediate and large x values. We should mention that this proof does not require a complete probabilistic picture of the evolution, but just the positivity of the bulk part of the kernels, the positivity of the edge point subtractions and their diagonality in flavour. From Figs. (2) and (5) it is also evident that the leading order kernels are positive, together with the qg and qq (Fig. (3)) sectors.

The edge point contributions, generating the “subtraction terms” in the master equations for the “ $++$ ” components of the kernels are positive, as is illustrated in 3 Tables included in Appendix A. There we have organized these terms in the form $\sim C\delta(1-x)$ with

$$C = -\log(1-\Lambda)A + B \quad (52)$$

with A and B being numerical coefficients depending on the number of flavours included in the kernels. Notice that the subtraction terms are always of the form (52), with the (diverging) logarithmic contribution ($\sim \int_0^\Lambda dz/(1-z)$) regulated by a cutoff. This divergence in the convolution cancels when these terms are combined with the divergence at $x=1$ of the first term of the master equation for all the relevant components containing “ $+$ ” distributions. It is crucial, however, to establish positivity of the evolution of the helicities that the boundary conditions on the evolution $|\Delta q(x, Q_0^2)| \leq q(x, Q_0^2)$ be satisfied. Initial conditions have this special property, in most of models, and the proof of positivity of all the distributions therefore holds at any Q .

As we move to NLO, the pattern gets more complicated. In fact, from a numerical check, one can see that some NLO kernels turn to be negative, including the unpolarized kernels and the helicity kernels, while others (Fig. (4)) are positive. One can also notice the presence of a crossing of several helicity components in the gq and gg sectors (see Fig. (7)) at larger x values, while in the small-x region some components turn negative (Fig. (6)). There is no compelling proof of positivity, in this case, either than that coming from a direct numerical analysis.

9 NLO Numerical Tests using Recursion Relations

We have seen that master forms of evolution equations, for evolutions of all kinds, when found, can be used to establish positivity of the evolution itself.

The requirements have been spelled out above and can be summarized in the following points: 1) diagonality of the decreasing terms, 2) initial positivity of the distributions, 3) positivity of the remaining (non diagonal) kernels. As we have also seen, some of these conditions are not satisfied by the NLO evolution.

In order then to proceed with a numerical test of the inequality we have decided to work directly in x-space, using a specific ansatz which summarizes the NLO evolution in a rather compact form.

This ansatz, which we will illustrate below, reduces the evolution equations to a suitable set of recursion relations [8], [9].

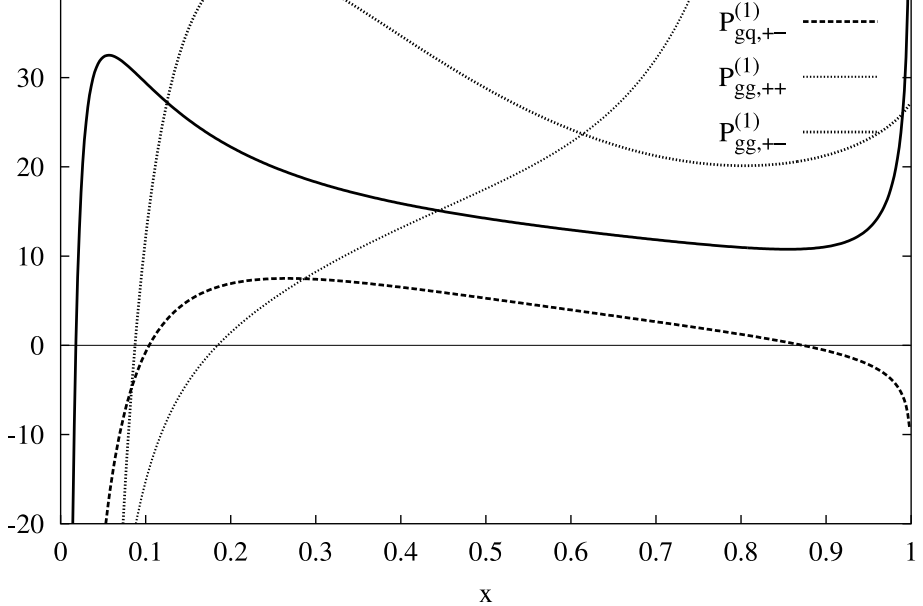


Figure 7: The crossing of NLO kernels (gq and gg) in the helicity basis.

In this ansatz, the NLO expansion of the distributions in the DGLAP equation is generically given by

$$f(x, Q^2) = \sum_{n=0}^{\infty} \frac{A_n(x)}{n!} \log^n \left(\frac{\alpha(Q^2)}{\alpha(Q_0^2)} \right) + \alpha(Q^2) \sum_{n=0}^{\infty} \frac{B_n(x)}{n!} \log^n \left(\frac{\alpha(Q^2)}{\alpha(Q_0^2)} \right) \quad (53)$$

where we assume a short hand matrix notation for all the convolution products. Notice that $f(x, Q^2)$ stands for a vector having as components all the helicities of the various flavours (q_{\pm}, G_{\pm}). The ansatz implies a tower of recursion relations once the running coupling is kept into account [10, 13]

The ansatz implies a tower of recursion relations once the running coupling is kept into account [10, 13]

$$A_{n+1}(x) = -\frac{2}{\beta_0} P^{(0)} \otimes A_n(x) \quad (54)$$

to leading order and

$$\begin{aligned} B_{n+1}(x) &= -B_n(x) - \left(\frac{\beta_1}{4\beta_0} A_{n+1}(x) \right) - \frac{1}{4\pi\beta_0} P^{(1)} \otimes A_n(x) - \frac{2}{\beta_0} P^{(0)} \otimes B_n(x) \\ &= -B_n(x) + \left(\frac{\beta_1}{2\beta_0^2} P^{(0)} \otimes A_n(x) \right) \\ &\quad - \frac{1}{4\pi\beta_0} P^{(1)} \otimes A_n(x) - \frac{2}{\beta_0} P^{(0)} \otimes B_n(x), \end{aligned} \quad (55)$$

to NLO, relations which are solved with the initial condition $B_0(x) = 0$. The initial conditions for the coefficients $A_0(x)$ and $B_0(x)$ are specified with $q(x, Q_0^2)$ as a leading order ansatz for the initial distribution

$$A_0(x) = \delta(1-x) \otimes q(x, Q_0^2) \equiv q_0(x) \quad (56)$$

$$A_0(x) + \alpha_0 B_0(x) = q_0(x). \quad (57)$$

Again, other boundary choices are possible for $A_0(x)$ and $B_0(x)$ as far as (57) is fulfilled.

Once the expansion is established, any linear combination of distributions has still to satisfy the same expansion, for appropriate combinations of the scale-invariant coefficients $A_n(x)$ given above. The positivity of the expansion, at least in leading order, is easy to establish. For this purpose consider the “++” or diagonal part of the recursion relations involving the coefficients

$$A_{n+1,+}(x) = -\frac{2}{\beta_0} P_{++}^{(0)} \otimes A_{n,+}(x) \quad (58)$$

and start from $n = 0$. Since $A_0(x)$ is the initial condition, it has to be positive by definition. The first iterate ($n = 1$) will then be negative by the same argument that forces $P_{++} \otimes A_0(x)$ to be positive. The signature of the recursion relations will then be equal to $(-1)^n$, and this factor is compensated by the other signature factor coming from the argument of the logarithm $(-1)^n$ since $\alpha/\alpha_0 < 1$ (asymptotic freedom). The argument does not work to NLO, and here only a numerical check provides insight on the signature of the coefficients $B_n(x)$ of the expansion.

10 Initial conditions and Results

As input distributions in the unpolarized case, we have used the parametrized formulas of Ref. [11], that are calculated to NLO in the $\overline{\text{MS}}$ scheme at a scale $Q_0^2 = 0.40 \text{ GeV}^2$

$$\begin{aligned} x(u - \bar{u})(x, Q_0^2) &= 0.632x^{0.43}(1 - x)^{3.09}(1 + 18.2x) \\ x(d - \bar{d})(x, Q_0^2) &= 0.624(1 - x)^{1.0}x(u - \bar{u})(x, Q_0^2) \\ x(\bar{d} - \bar{u})(x, Q_0^2) &= 0.20x^{0.43}(1 - x)^{12.4}(1 - 13.3\sqrt{x} + 60.0x) \\ x(\bar{u} + \bar{d})(x, Q_0^2) &= 1.24x^{0.20}(1 - x)^{8.5}(1 - 2.3\sqrt{x} + 5.7x) \\ xg(x, Q_0^2) &= 20.80x^{1.6}(1 - x)^{4.1} \end{aligned} \quad (59)$$

and $xq_i(x, Q_0^2) = x\bar{q}_i(x, Q_0^2) = 0$ for $q_i = s, c, b, t$.

Following [12], we have related the unpolarized input distributions to the longitudinally polarized ones by

$$\begin{aligned} x\Delta u(x, Q_0^2) &= 1.019x^{0.52}(1 - x)^{0.12}xu(x, Q_0^2) \\ x\Delta d(x, Q_0^2) &= -0.669x^{0.43}xd(x, Q_0^2) \\ x\Delta \bar{u}(x, Q_0^2) &= -0.272x^{0.38}x\bar{u}(x, Q_0^2) \\ x\Delta \bar{d}(x, Q_0^2) &= x\Delta \bar{u}(x, Q_0^2) \\ x\Delta g(x, Q_0^2) &= 1.419x^{1.43}(1 - x)^{0.15}xg(x, Q_0^2) \end{aligned} \quad (60)$$

and $x\Delta q_i(x, Q_0^2) = x\Delta \bar{q}_i(x, Q_0^2) = 0$ for $q_i = s, c, b, t$.

We show in Fig. 8 results for the evolution of the u^+ distribution at the initial scale (0.632 GeV) and at two final scales, 100 GeV and 200 GeV respectively. The peaks at the

Q increases. In Fig. 9 u^- show an apparent steeper growth at small- x compared to u^+ . For the d distributions the situation is inverted, with d^- growing steeper compared to d^+ (Figs. 11 and 12 respectively). This apparent behaviour is resolved in Figs. (10) and (13) from which it is evident that both plus and minus components converge, at very small- x values, toward the same limit.

The components s, c, t and b (Figs. 14-21) have been generated radiatively from vanishing initial conditions for final evolution scales of 100 and 200 GeV (s, c, b) and 200 GeV (t).

Both positive and negative components grow steadily at small- x and are negligible at larger x values. The distribution for the top (t) has been included for completeness. Given the smaller evolution interval the helicity distributions for heavier generations are suppressed compared to those of lighter flavours. Gluon helicities (Figs. 22 23) are also enhanced at small- x , and show a similar growth. The fine difference between the quark u and d distributions are shown in Figs. 10 and 13.

Finally in Figs. 24, 25 and 26 we plot simultaneously longitudinally polarized, unpolarized and helicity distributions for up quarks, down quarks and gluons at an intermediate factorization scale of 100 GeV, relevant for experiments at RHIC. Notice that while u^+ and u^- are positive and their difference (Δu) is also positive, for down quarks the two helicity components are positive while their difference (Δd) is negative. Gluons, in the model studied here, have a positive longitudinal polarization, and the helicity components are also positive. The positive and negative gluon helicities are plotted in a separate figure, Fig. 22 and 23, while their difference, $\Delta g(x)$ is shown in Fig. 27. One can observe, at least in this model, a crossing at small- x in this distribution.

We conclude that, at least for this set of boundary conditions, positivity of all the components holds to NLO, as expected.

11 Conclusions

We have discussed in detail some of the main features of the probabilistic approach to the DGLAP evolution in the helicity basis. Numerical results for the evolution of all the helicities have been provided, using a special algorithm, based in x -space. We have also illustrated some of the essential differences between the standard distributional form of the kernels and their probabilistic version, clarifying some issues connected to their regularization. Then we have turned to the probabilistic picture, stressing on the connection between the random walk approach to parton diffusion in x -space and the master form of the DGLAP equation. The link between the two descriptions has been discussed especially in the context of the Kramers-Moyal expansion. A Fokker-Planck approximation to the expansion has also been presented which may turn useful for the study of formal properties of the probabilistic evolution. We have also seen that positivity of the helicity distributions, to NLO, requires a numerical analysis, as already hinted in [2]. Our study also validates the use of a very fast evolution algorithm, alternative to other standard algorithms based on Mellin algorithms, whose advantage is especially in the analysis of the evolution of nonforward parton distributions, as we will show elsewhere.

We thank O. Teryaev for correspondence and the IFT at the Univ. of Florida for hospitality and INFN of Italy (BA-21) for partial financial support.

A Edge Point Positivity

We report below 3 tables illustrating the (positive) numerical values of the contributions coming from the subtraction terms in the NLO kernels. Coefficients A and B refer to the subtraction terms $-\log(1 - \Lambda)A + B$ as explained in the section above.

N_f	A	B
3	12.5302	12.1739
4	10.9569	10.6924
5	9.3836	9.2109
6	7.8103	7.7249

Table 1. Coefficients A and B as in Table 1 for $P_{NS,++}^{(1)}$

N_f	A	B
3	12.5302	12.1739
4	10.9569	10.6924
5	9.3836	9.2109
6	7.8103	7.7249

Table 2. Coefficients A and B as in Table 1 for $P_{qq,++}^{(1)}$

N_f	A	B
3	48.4555	27.3912
4	45.7889	24.0579
5	43.1222	20.7245
6	40.4555	17.3912

Table 3. Coefficients A and B as in Table 1 for $P_{gg,++}^{(1)}$

B Regularizations

The “+” plus form of the kernels and all the other forms introduced before, obtained by separating the contributions from the edge-point ($x = 1$) from those coming from the bulk ($0 < x < 1$) are all equivalent, as we are going to show, with the understanding that a linear (unique) cutoff is used to regulate the divergences both at $x=0$ and at $x=1$. We focus here on the two possible sources of singularity, i.e. on P_{qq} and on the P_{gg} contributions, which require some attention. Let’s start from the P_{qq} case. We recall that “+” plus distributions are defined as

$$\frac{1}{(1-x)_+} = \frac{\theta(1-x-\Lambda)}{1-x} - \delta(1-x) \int_0^{1-\Lambda} \frac{dz}{1-z} \quad (61)$$

with Λ being a cutoff for the edge-point contribution.

We will be using the relations

$$\begin{aligned} \int_x^1 \frac{dy}{y} \delta(1-y) &= 1 \\ \int_0^1 \frac{dz}{1-z} &= \int_x^1 \frac{dz}{1-z} - \log(1-x) \\ \int_x^1 \frac{dy}{y} f(y) g(x/y) &= \int_x^1 \frac{dy}{y} f(x/y) g(y). \end{aligned} \quad (62)$$

$$\begin{aligned}
\frac{1}{(1-x)_+} \otimes f(x) &= \int_x^1 \frac{dy}{y} \frac{1}{(1-x/y)_+} q(y) \\
&= \int_x^1 \frac{dy}{y} \frac{1}{1-x/y} f(y) - \int_x^1 \frac{dy}{y} \delta(1-y) \int_0^1 \frac{dz}{z} \\
&= \int_x^1 \frac{dy}{y} \frac{yf(y) - xf(x)}{y-x} + \log(1-x) f(x)
\end{aligned} \tag{63}$$

which is eq. (18). If we remove the “+” distributions and adopt (implicitly) a cutoff regularization, we need special care. In the probabilistic version of the kernel, the handling of $P_{qq} \otimes q$ is rather straightforward

$$\begin{aligned}
P_{qq} \otimes q(x) &= C_F \int_x^1 \frac{dy}{y} \left(\frac{2}{1-x/y} - 1 - x/y \right) q(y) \\
&\quad - C_F \int_x^1 \frac{dy}{y} \delta(1-y) \int_0^1 dz' \left(\frac{2}{1-z'} - 1 - z' \right)
\end{aligned} \tag{64}$$

and using eqs. (62) we easily obtain

$$\begin{aligned}
P_{qq} \otimes q(x) &= 2C_F \int_x^1 \frac{dy}{y} \frac{yq(y) - xq(x)}{y-x} - 2C_F \log(1-x) q(x) \\
&\quad - C_F \int_x^1 \frac{dy}{y} (1+x/y) q(y) + \frac{3}{2} C_F q(x).
\end{aligned} \tag{65}$$

Now consider the convolution $P_{gg} \otimes g(x)$ in the Collins-Qiu form. We get

$$\begin{aligned}
P_{gg} \otimes g(x) &= 2C_A \int_x^1 y \frac{dy}{y} \frac{1}{1-x/y} g(y) \\
&\quad + 2C_A \int_x^1 \frac{dy}{y} \left(x/y(1-x/y) + \frac{1}{x/y} - 2 \right) g(y) - \frac{1}{2} g(x) \int_0^1 \frac{dz}{2} C_A \left(\frac{1}{z} + \frac{1}{1-z} \right) \\
&\quad - \frac{1}{2} g(x) \int_0^1 dz 2C_A (z(1-z) - 2) - n_f g(x) \int_0^1 dz \frac{1}{2} (z^2 + (1-z)^2).
\end{aligned} \tag{66}$$

There are some terms in the expression above that require some care. The appropriate regularization is

$$\int_0^1 \frac{dz}{z} + \int_0^1 \frac{dz}{1-z} \rightarrow I(\Lambda) = \int_\Lambda^1 \frac{dz}{z} + \int_0^{1-\Lambda} \frac{dz}{1-z}. \tag{67}$$

Observe also that

$$\int_\Lambda^1 \frac{dz}{z} = \int_0^{1-\Lambda} \frac{dz}{1-z} = -\log \Lambda. \tag{68}$$

Notice that in this regularization the singularity of $1/z$ at $z=0$ is traded for a singularity at $z=1$ in $1/(1-z)$. It is then rather straightforward to show that

$$\begin{aligned}
P_{qq} \otimes g(x) &= 2C_A \int_x^1 \frac{dy}{y} \frac{yg(y) - xg(x)}{y-x} - 2C_A \log(1-x) g(x) \\
&\quad + 2C_A \int_x^1 \frac{dy}{y} \left(x/y(1-x/y) + \frac{1}{x/y} - 2 \right) + \frac{\beta_0}{2} g(x).
\end{aligned} \tag{69}$$

$$\int_0^1 dz (z - \frac{1}{2}) \gamma_{gg} = 0 \quad (70)$$

that we need to check with the regularization given above.

The strategy to handle this expression is the same as before. We extract all the $1/z$ and $1/(1-z)$ integration terms and use

$$\begin{aligned} \int_0^1 \frac{dz}{z} - \int_0^1 \frac{dz}{1-z} &\rightarrow \int_{\Lambda}^1 \frac{dz}{z} - \int_0^{1-\Lambda} \frac{dz}{1-z} \\ &= -\log \Lambda + \log (1-\Lambda) = 0 \end{aligned} \quad (71)$$

to eliminate the singularities at the boundaries $x = 0, 1$ and verify eq. (70).

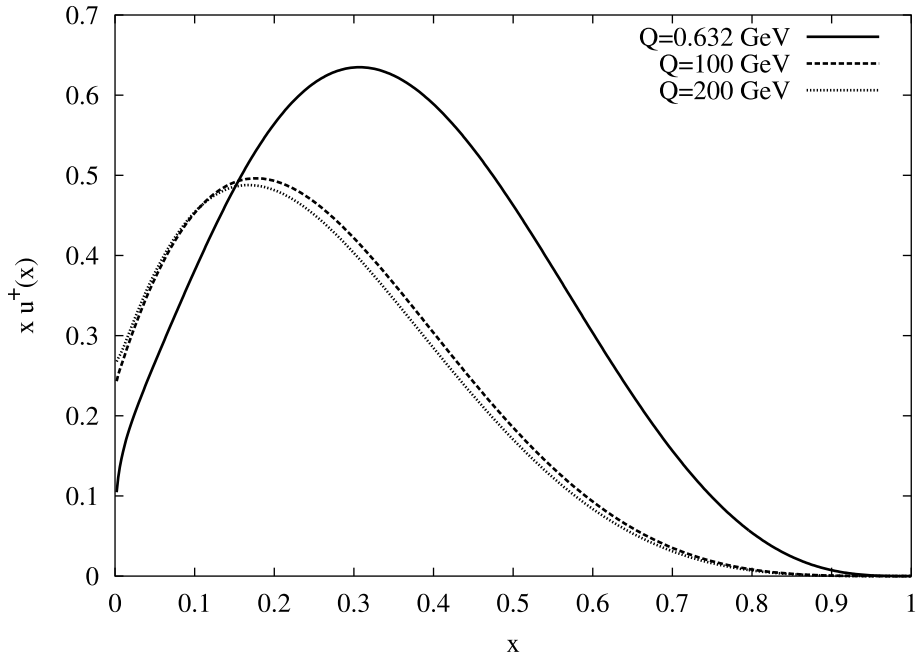


Figure 8: Evolution of u^+ versus x at various Q values.

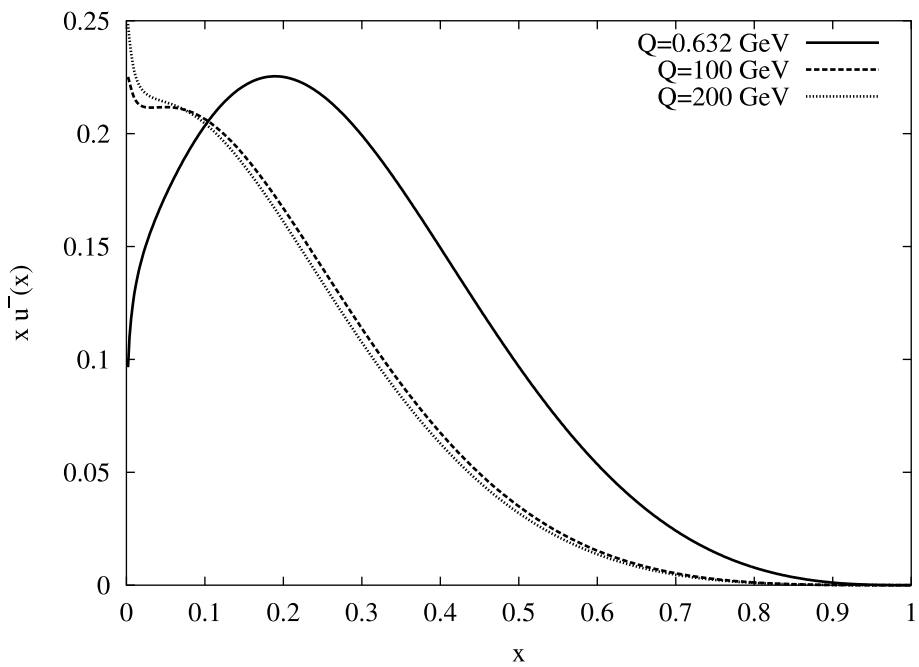


Figure 9: Evolution of u^- versus x at various Q values.

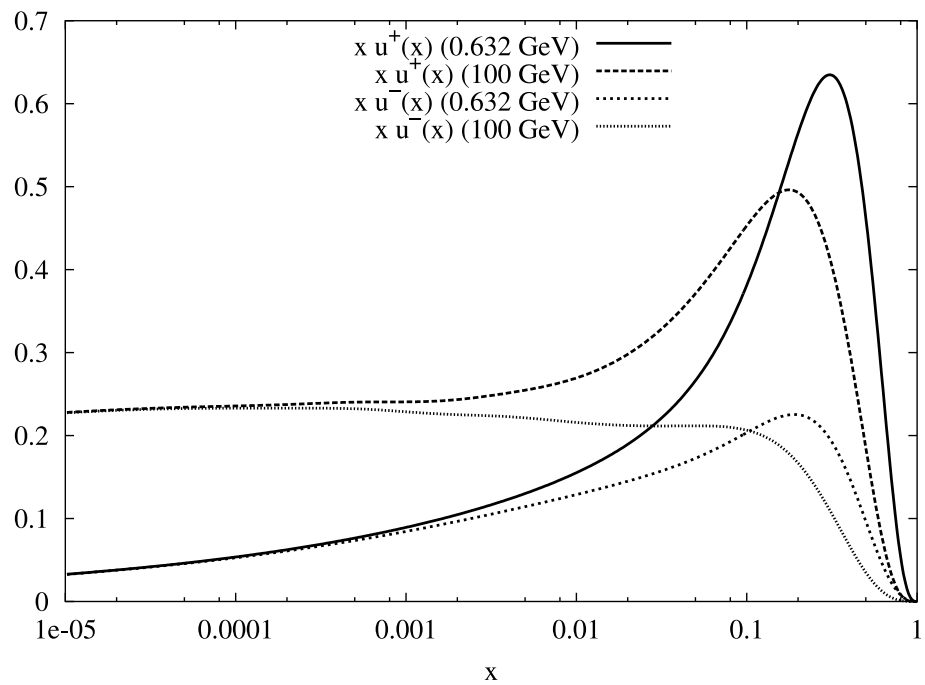


Figure 10: Small- x behaviour of u^\pm at 100 GeV.

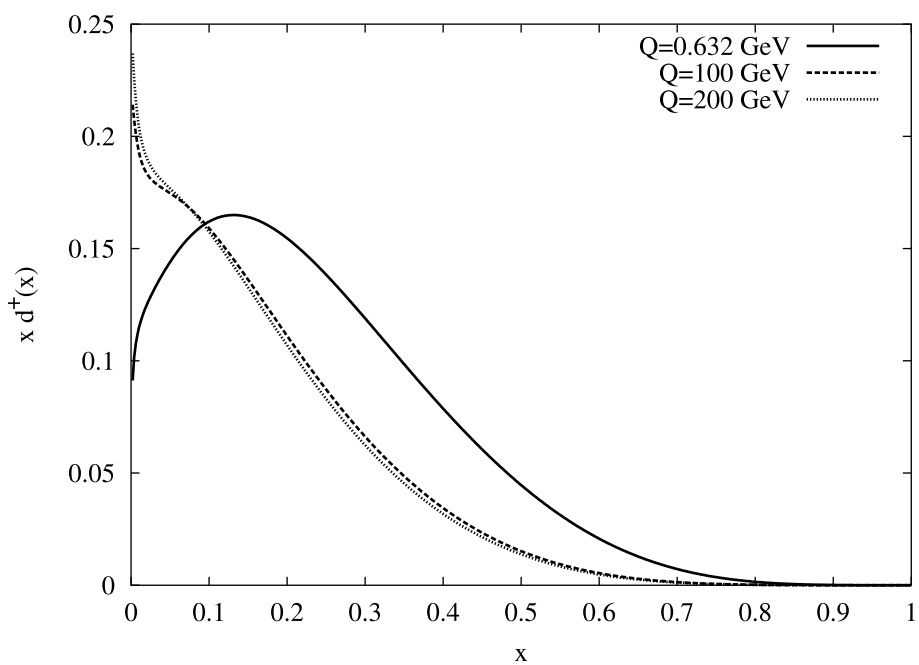


Figure 11: Evolution of d^+ versus x at various Q values.

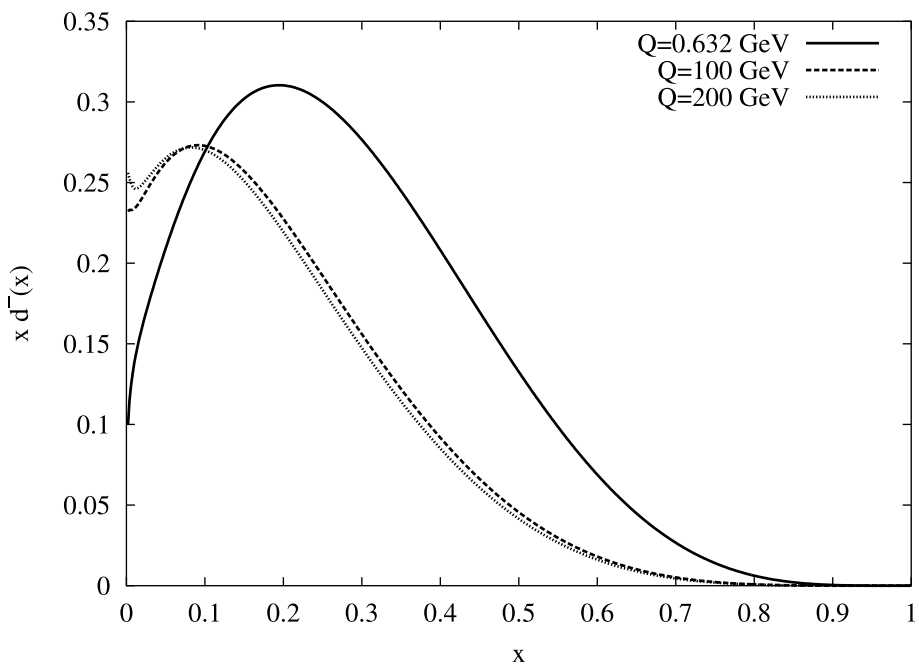


Figure 12: Evolution of d^- versus x at various Q values.

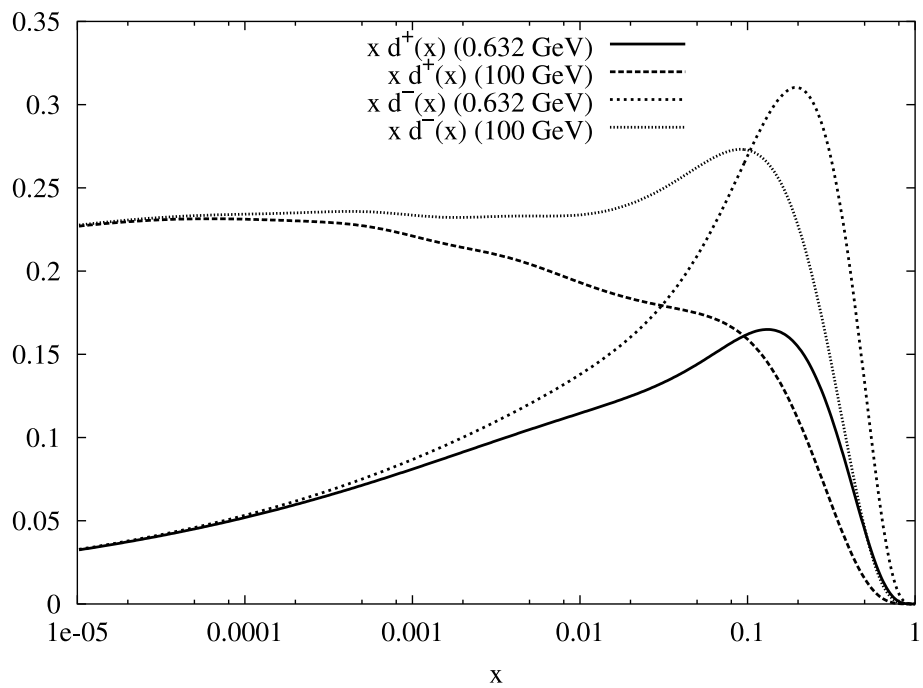


Figure 13: Small- x behaviour of d^\pm at 100 GeV.

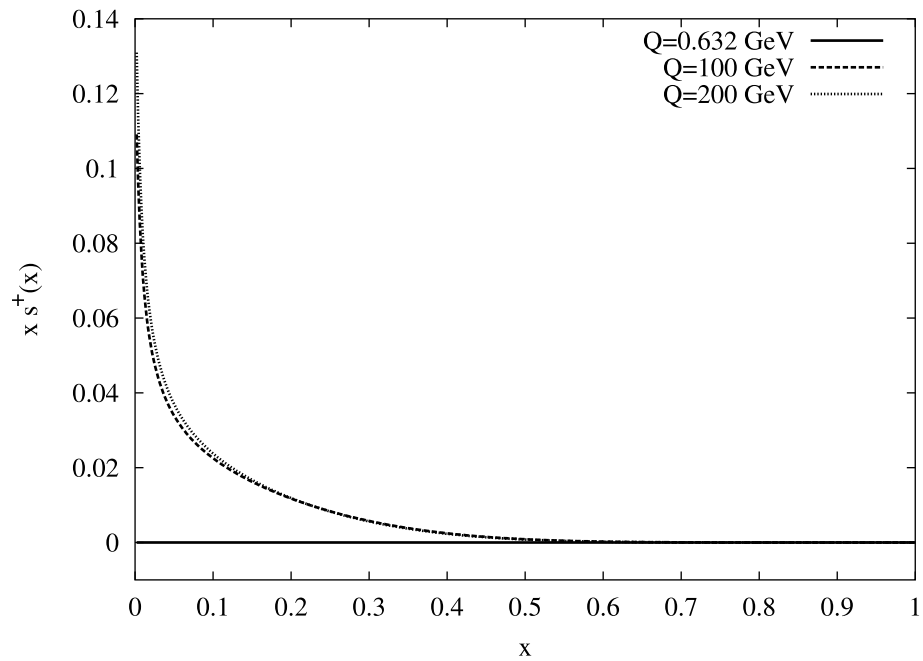


Figure 14: Evolution of s^+ versus x at various Q values.

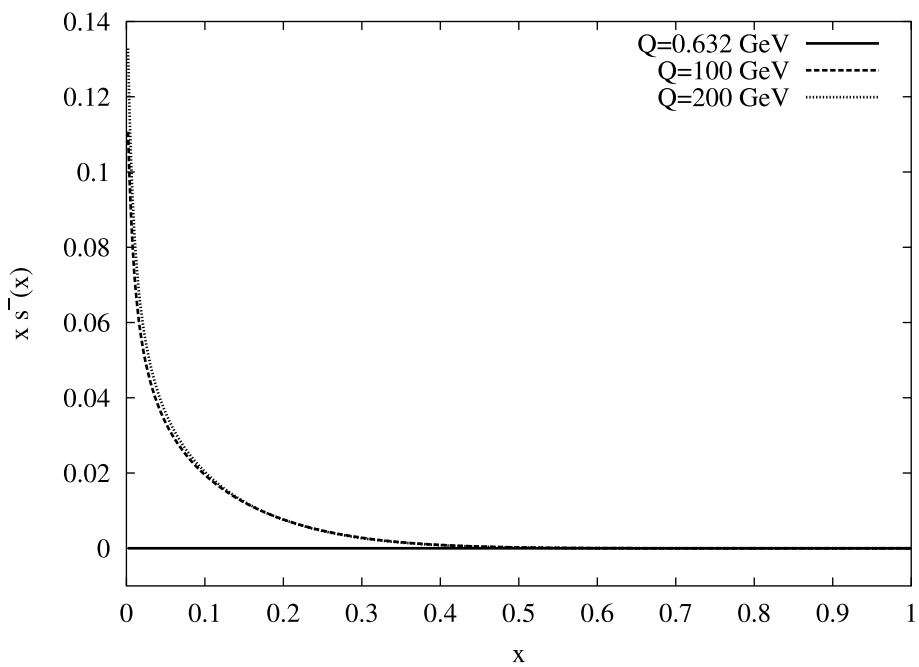


Figure 15: Evolution of s^- versus x at various Q values.

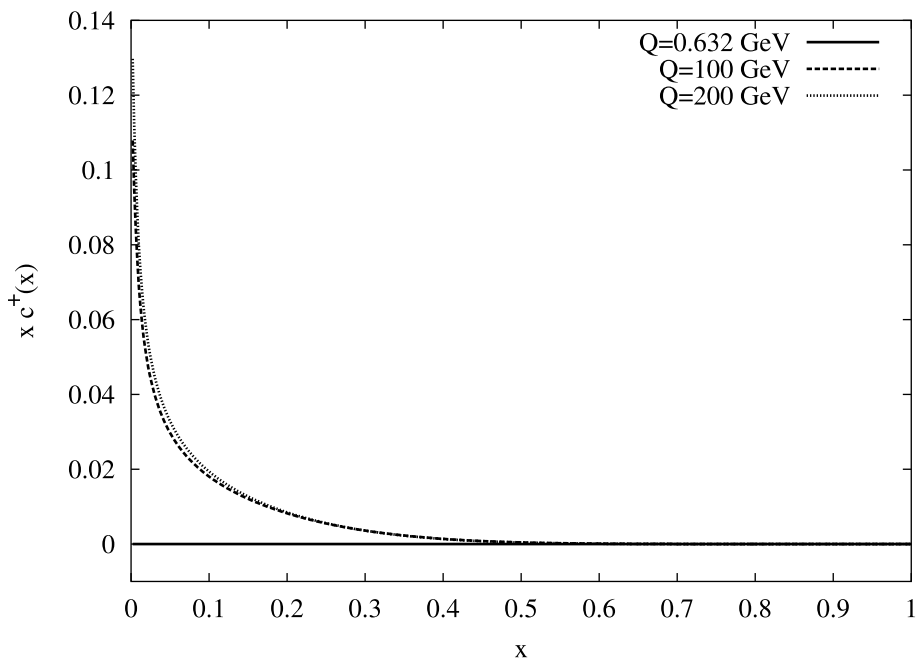


Figure 16: Evolution of c^+ versus x at various Q values.

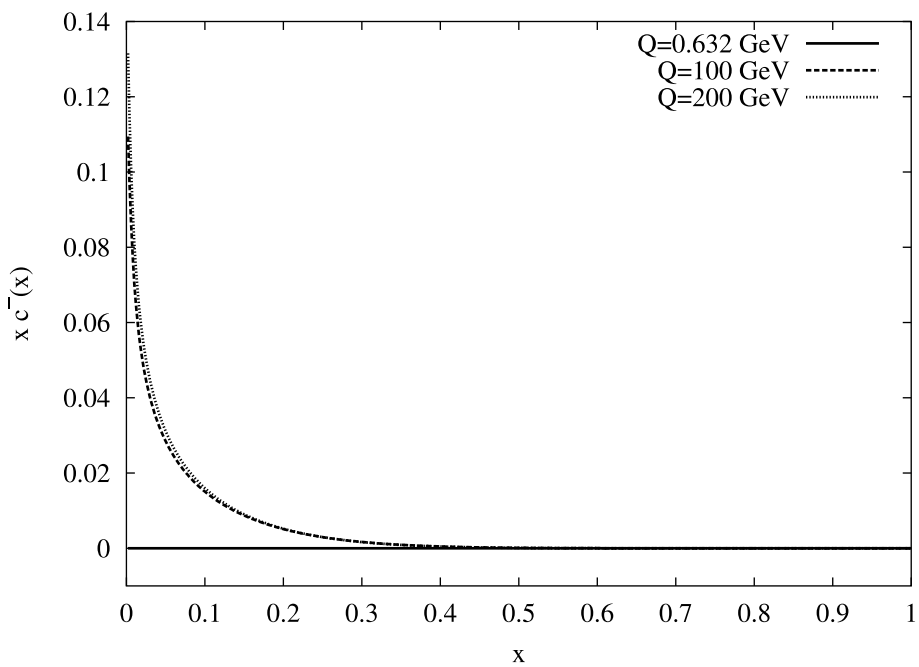


Figure 17: Evolution of c^- versus x at various Q values.

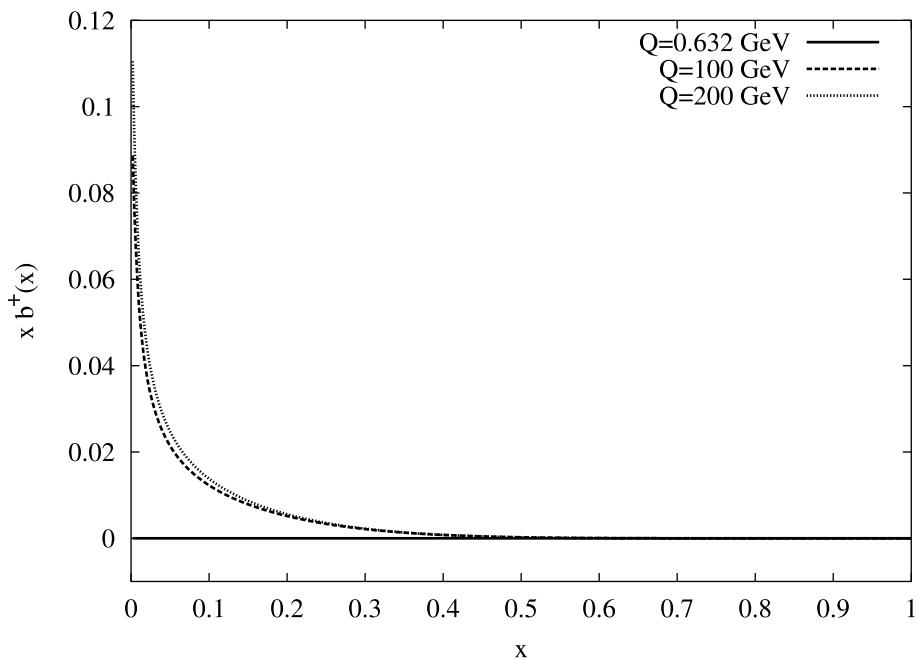


Figure 18: Evolution of b^+ versus x at various Q values.

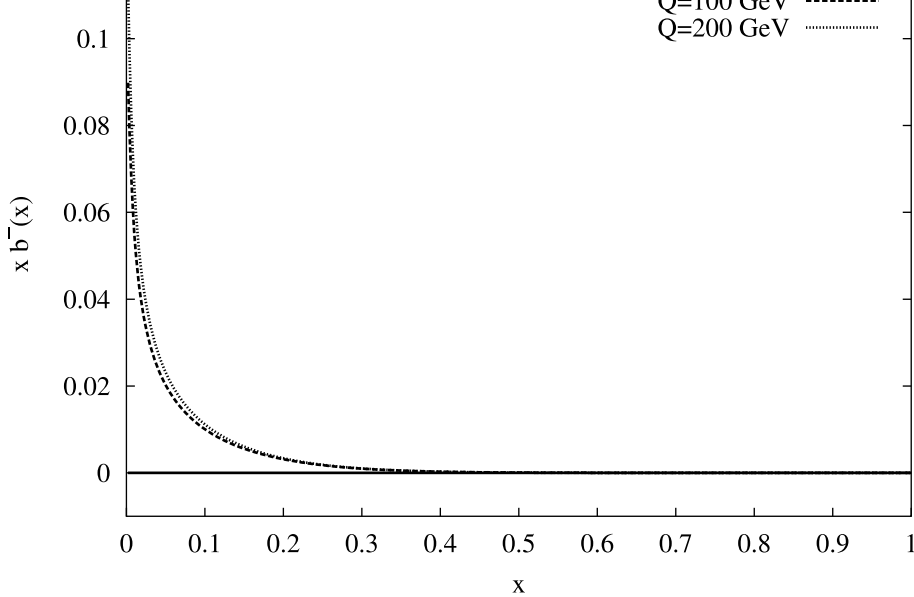


Figure 19: Evolution of b^- versus x at various Q values.

C Kernels in the helicity basis

The expression of the kernels in the helicity basis given below are obtained combining the NLO computations of [17, 16, 18]

$$\begin{aligned}
P_{NS^-,++}^{(1)}(x) = & \left\{ \frac{C_F}{18} \left[90C_F(x-1) + 4T_f(11x-1) + N_C(53 - 187x + 3\pi^2(1+x)) \right] \right\} \\
& + \left\{ \frac{C_F [6C_F(3 - 2(x-1)x) + 4T_f(1+x^2) - N_C(17 + 5x^2)]}{6(x-1)} \right\} \log x \\
& + \left\{ \frac{C_F [C_F - N_C - (C_F + N_C)x^2]}{2(x-1)} \right\} \log^2 x \\
& + \left\{ \frac{2C_F^2(1+x^2)}{x-1} \right\} \log x \log(1-x) \\
& + \left\{ -\frac{C_F}{9} [N_C(3\pi^2 - 67) + 20T_f] \right\} \frac{1}{(1-x)_+} \\
& + \left\{ C_F \left[\frac{N_C(51 + 44\pi^2) - 4T_f(3 + 4\pi^2)}{72} - 3N_C\zeta(3) \right. \right. \\
& \quad \left. \left. + C_F \left(\frac{3}{8} - \frac{\pi^2}{2} + 6\zeta(3) \right) \right] \right\} \delta(1-x) \tag{72}
\end{aligned}$$

$$\begin{aligned}
P_{NS^-,+-}^{(1)}(x) = & \{2C_F(2C_F - N_C)(x-1)\} \\
& + \{C_F(N_C - 2C_F)(1+x)\} \log x \\
& + \left\{ \frac{C_F(N_C - 2C_F)(1+x^2)}{1+x} \right\} S_2(x) \tag{73}
\end{aligned}$$

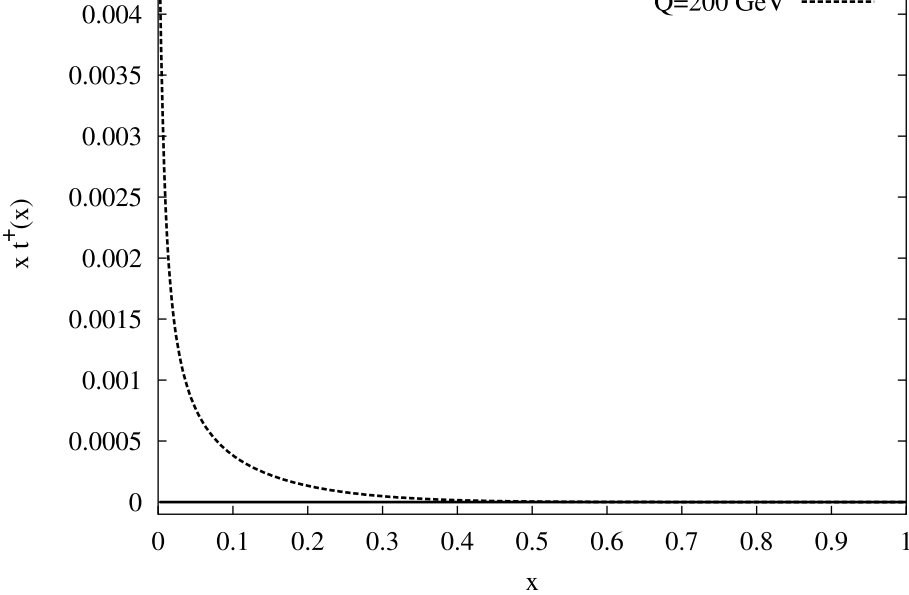


Figure 20: Evolution of t^+ versus x at various Q values.

$$P_{NS^+,++}^{(1)}(x) = P_{NS^-,++}^{(1)}(x) \quad (74)$$

$$P_{NS^+,+-}^{(1)}(x) = -P_{NS^-,+-}^{(1)}(x) \quad (75)$$

$$\begin{aligned}
P_{qq,++}^{(1)}(x) = & \left\{ \frac{C_F}{18x} [2T_f(20 - (x-1)x(56x-11)) \right. \\
& \left. + x(90C_F(x-1) + N_C(53 - 187x + 3\pi^2(1+x)))] \right\} \\
& + \left\{ \frac{C_F}{6(x-1)} [6C_F(3 - 2(x-1)x) - N_C(17 + 5x^2) \right. \\
& \left. + 4T_f(1 + x(x(9 + 4x) - 12))] \right\} \log x \\
& + \left\{ \frac{C_F [C_F - N_C + 4T_f - (C_F + N_C + 4T_F)x^2]}{2(x-1)} \right\} \log^2 x \\
& + \left\{ \frac{2C_F^2(1+x^2)}{x-1} \right\} \log x \log(1-x) \\
& + \left\{ -\frac{C_F}{9} [N_C(3\pi^2 - 67) + 20T_f] \right\} \frac{1}{(1-x)_+} \\
& + \left\{ \frac{C_F}{72} [N_C(51 + 44\pi^2 - 216\zeta(3)) - 4T_f(3 + 4\pi^2) \right. \\
& \left. + 9C_F(3 - 4\pi^2 + 48\zeta(3))] \right\} \delta(1-x) \quad (76)
\end{aligned}$$

$$\begin{aligned}
P_{qq,+-}^{(1)}(x) = & \left\{ \frac{C_F(1-x)}{9x} [18(2C_F - N_C)x + T_f(20 - 7x + 56x^2)] \right\} \\
& + \left\{ \frac{C_F}{3} [6C_F(1+x) - 3N_C(1+x) + 2T_f(3 + x(3 + 4x))] \right\} \log x \\
& + \left\{ \frac{C_F(2C_F - N_C)(1+x^2)}{1+x} \right\} S_2(x) \quad (77)
\end{aligned}$$

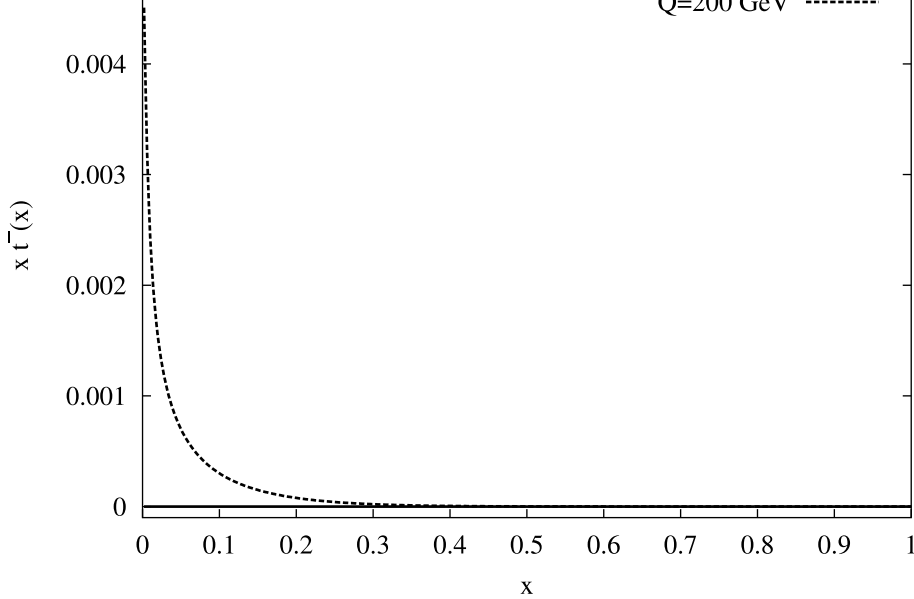


Figure 21: Evolution of t^- versus x at various Q values.

$$\begin{aligned}
P_{qg,++}^{(1)}(x) = & \left\{ \frac{T_f}{9x} \left[N_C(20 + x(90 + x(126 + (3\pi^2 - 218)x))) \right. \right. \\
& \left. \left. - 3C_Fx(12 - x(2(15 - \pi^2)x - 3)) \right] \right\} \\
& + \left\{ \frac{T_f}{3} \left[6N_C + 4N_Cx(12 + 11x) - 3C_F(3 + 2x - 4x^2) \right] \right\} \log x \\
& + \left\{ 4T_f(C_F - N_C)(1 - x^2) \right\} \log(1 - x) \\
& + \left\{ T_f \left[2C_Fx^2 - N_C(3 + x(6 + x)) \right] \right\} \log^2 x \\
& + \left\{ 2T_f(C_F - N_C)x^2 \right\} \log^2(1 - x) \\
& + \left\{ -4C_FT_fx^2 \right\} \log x \log(1 - x) \\
& + \left\{ 2N_C T_f(1 + x)^2 \right\} S_2(x)
\end{aligned} \tag{78}$$

$$\begin{aligned}
P_{qg,+-}^{(1)}(x) = & \left\{ \frac{T_f(x-1)}{9x} \left[6C_Fx(15x - 27 - \pi^2(x-1)) \right. \right. \\
& \left. \left. - N_C(20 - (106 + 3\pi^2(x-1) - 218x)x) \right] \right\} \\
& + \left\{ \frac{2}{3}T_f \left[22N_Cx^2 + 3C_F(3 + x(2x-1)) \right] \right\} \log x \\
& + \left\{ 4T_f(N_C - C_F)(1 - x)^2 \right\} \log(1 - x) \\
& + \left\{ T_f \left[C_F(1 + 2(x-1)x) - N_Cx^2 \right] \right\} \log^2 x \\
& + \left\{ 2T_f(C_F - N_C)(1 - x)^2 \right\} \log^2(1 - x) \\
& + \left\{ -4C_FT_fx^2 \right\} \log x \log(1 - x) \\
& + \left\{ 2N_C T_fx^2 \right\} S_2(x)
\end{aligned} \tag{79}$$

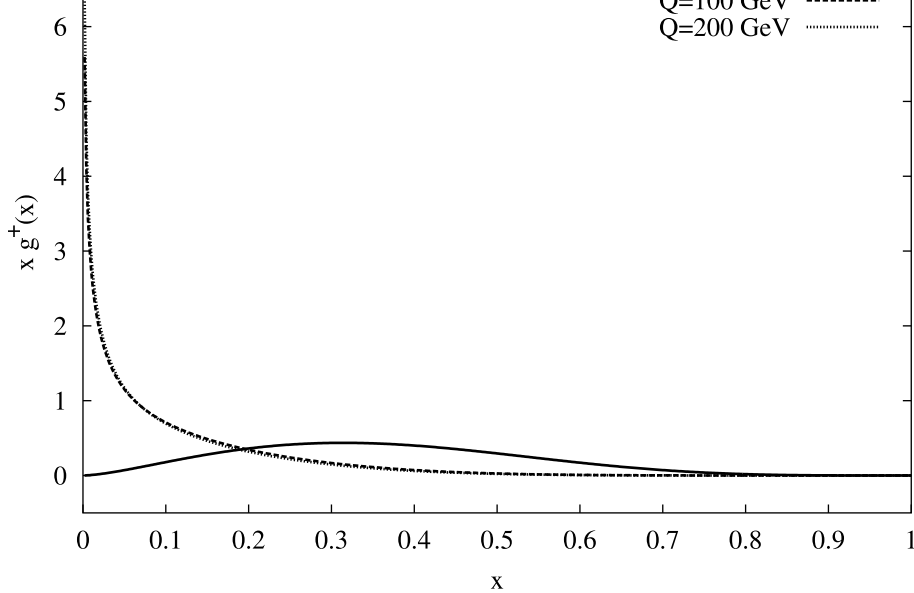


Figure 22: Evolution of g^+ versus x at various Q values.

$$\begin{aligned}
P_{gq,++}^{(1)}(x) = & \left\{ \frac{C_F}{36x} [9C_F(x-22)x - 8T_f(10 + 3x(3x-2)) \right. \\
& \left. + 2N_C(9 - 3\pi^2 + 4x(15 + x(18 + 11x)))] \right\} \\
& + \left\{ \frac{C_F}{3} [6C_Fx - N_C(12 + x(27 + 4x))] \right\} \log x \\
& + \left\{ \frac{C_F}{3x} [N_C(11 - 3(2 - 3x)x) - 4T_f - 3C_F(3 + x(3x - 2))] \right\} \log(1 - x) \\
& + \left\{ \frac{C_F N_C(1 + 3x(2 + x))}{2x} \right\} \log^2 x \\
& + \left\{ \frac{C_F(N_C - C_F)}{x} \right\} \log^2(1 - x) \\
& + \left\{ -\frac{2C_F N_C}{x} \right\} \log x \log(1 - x) \\
& + \left\{ -\frac{C_F N_C(1 + x)^2}{x} \right\} S_2(x)
\end{aligned} \tag{80}$$

$$\begin{aligned}
P_{gq,+-}^{(1)}(x) = & \left\{ \frac{C_F}{36x} [27C_F(4 - 5x)x - 8T_f(10 + 7(x - 2)x) \right. \\
& \left. + 2N_C(9 - 3\pi^2(x - 1)^2 - 2x(11 - x - 22x^2))] \right\} \\
& + \left\{ \frac{C_F}{6} [3C_F(4 + 3x) - 8N_C(6 + (x - 3)x)] \right\} \log x \\
& + \left\{ \frac{C_F}{3x} [N_C(11 + 8(x - 2)x) - 4T_f(1 - x)^2 \right. \\
& \left. - 3C_F(3 + 2(x - 2)x)] \right\} \log(1 - x) \\
& + \left\{ \frac{C_F}{2x} [N_C + C_F(x - 2)x] \right\} \log^2 x
\end{aligned}$$

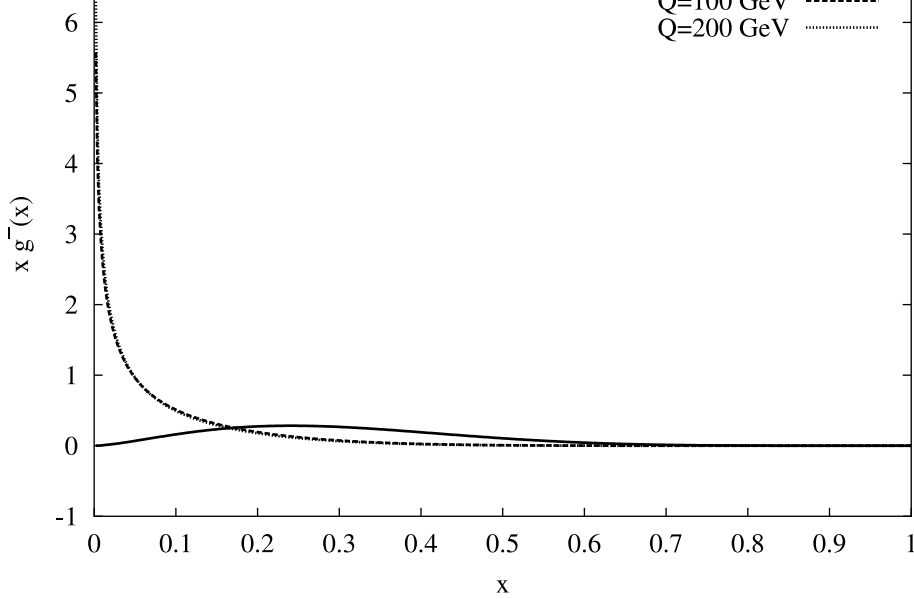


Figure 23: Evolution of g^- versus x at various Q values.

$$\begin{aligned}
& + \left\{ -\frac{C_F(C_F - N_C)(x-1)^2}{x} \right\} \log^2(1-x) \\
& + \left\{ -\frac{2C_F N_C (x-1)^2}{x} \right\} \log x \log(1-x) \\
& + \left\{ -\frac{C_F N_C}{x} \right\} S_2(x)
\end{aligned} \tag{81}$$

$$\begin{aligned}
P_{gg,++}^{(1)}(x) = & \left\{ \frac{1}{18x} [6C_F T_f(x-1)(x(37+10x)-2) \right. \\
& + 2C_F T_f(x(21+x(19+23x))-23) \\
& \left. + N_C^2(3\pi^2(x(3+x+x^2)-1)-x(165+103x))] \right\} \\
& + \left\{ -\frac{2}{3} [2N_C T_f(1+x) + 6C_F T_f(2+x) + N_C^2(x(14+11x)-1)] \right\} \log x \\
& + \left\{ \frac{4C_F T_f x(x^2-1) + N_C^2(1+x(6+x(2+(x-8)x)))}{2(1-x)x} \right\} \log^2 x \\
& + \left\{ \frac{2N_C^2(1-x(2-2x-x^3))}{(x-1)x} \right\} \log x \log(1-x) \\
& + \left\{ -\frac{N_C^2(1+x+3x^2+x^3)}{x} \right\} S_2(x) \\
& + \left\{ \frac{N_C}{9} [N_C(67-3\pi^2) - 20T_f] \right\} \frac{1}{(1-x)_+} \\
& + \left\{ N_C^2 \left(\frac{8}{3} + 3\zeta(3) \right) - C_F T_f - \frac{4N_C T_f}{3} \right\} \delta(1-x)
\end{aligned} \tag{82}$$

$$P_{gg,+-}^{(1)}(x) = \left\{ \frac{1}{18x} [6C_F T_f(x-1)(x(7+10x)-2) \right.$$

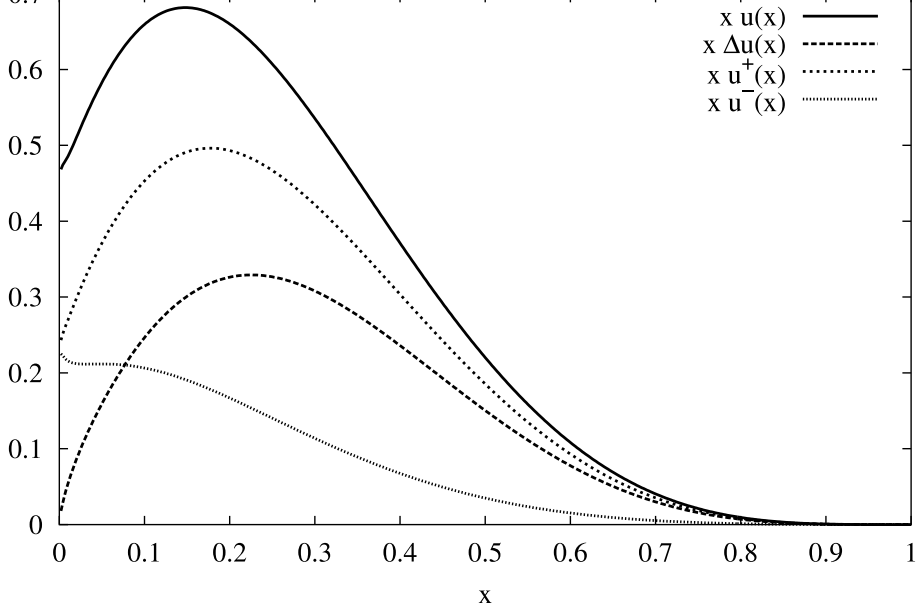


Figure 24: Various kinds of distributions of quark up at $Q = 100$ GeV.

$$\begin{aligned}
& + N_C^2 (2(70 - 3x)x - 3\pi^2(1 - x + 3x^2 - x^3)) \\
& + 2N_C T_f (x(37 + x(23x - 57)) - 23) \} \\
& + \left\{ 2C_F T_f (1 - 3x) - N_C^2 \left(9 - 13x + \frac{22x^2}{3} \right) \right\} \log x \\
& + \left\{ \frac{N_c^2}{2x} (1 - x + 3x^2 - x^3) \right\} \log^2 x \\
& + \left\{ \frac{2N_C^2}{x} (x^3 - 3x^2 + x - 1) \right\} \log x \log(1 - x) \\
& + \left\{ -\frac{N_C^2(1 + x(2 + 2x + x^3))}{x(1 + x)} \right\} S_2(x) \tag{83}
\end{aligned}$$

References

- [1] J.C. Collins and J. Qiu, Phys.Rev.D39 1398,1989.
- [2] C. Bourrely, E. Leader, O.V. Teryaev, hep-ph/9803238.
- [3] C. Bourrely, J. Soffer, O.V. Teryaev, Phys.Lett.B420 375,1998.
- [4] D. Boyanovsky, H.J. De Vega, D.S. Lee, S.Y. Wang, H.L. Yu, Phys.Rev.D65 045014,2002.
- [5] B. E. Baaquie, C. Corianó and S. Marakani, cond-mat/0211489.
- [6] E. Eichten (Fermilab), I. Hinchliffe, Kenneth D. Lane and C. Quigg, Rev.Mod.Phys.56, 579, 1984.
- [7] M.Gluck, E.Reya and A.Vogt, Eur.Phys.J.C 5 (1998) 461

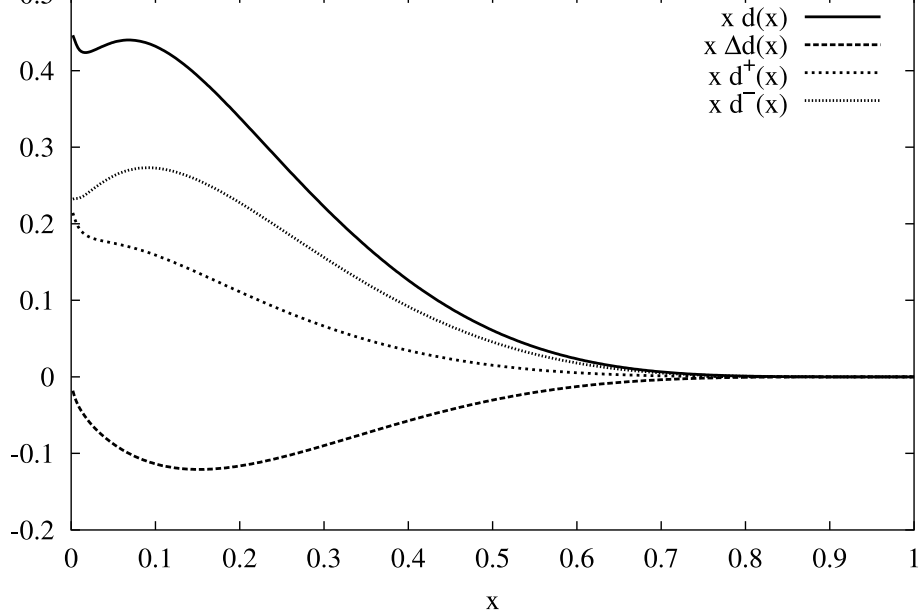


Figure 25: Various kinds of distributions of quark down at $Q = 100$ GeV.

- [8] G. Rossi, Phys.Rev.D29:852, 1984.
- [9] J.H. Da Luz Vieira, J.K. Storrow, Z.Phys.C51 241,1991.
- [10] L.E. Gordon and G. P. Ramsey Phys.Rev.D58 094017, 1998.
- [11] M.Gluck, E.Reya and A.Vogt, Eur.Phys.J.C 5, 461, 1998.
- [12] M.Gluck, E.Reya, M.Stratmann and W.Vogelsang, Phys.Rev.D 63 094005, 2001.
- [13] A. Cafarella, C. Corianò and M. Guzzi, hep-ph/0209149, Proceedings of the Intl. Workshop on Nonlinear Physics, ed. B. Prinari et. al., World Scientific 2003 (in press).
- [14] O.Martin, A.Schafer, M.Stratmann and W.Vogelsang, Phys.Rev.D 57 1117502, 1998.
- [15] A. Cafarella, C. Corianò, in preparation.
- [16] G. Curci, W. Furmanski and R. Petronzio, Nucl.Phys.B175:27, 1980
- [17] R. Mertig and W. L. Van Neerven, Z.Phys.C70 637, 1996.
- [18] W. Vogelsang, Nucl.Phys.B475, 47, 1996.

Q=100 GeV

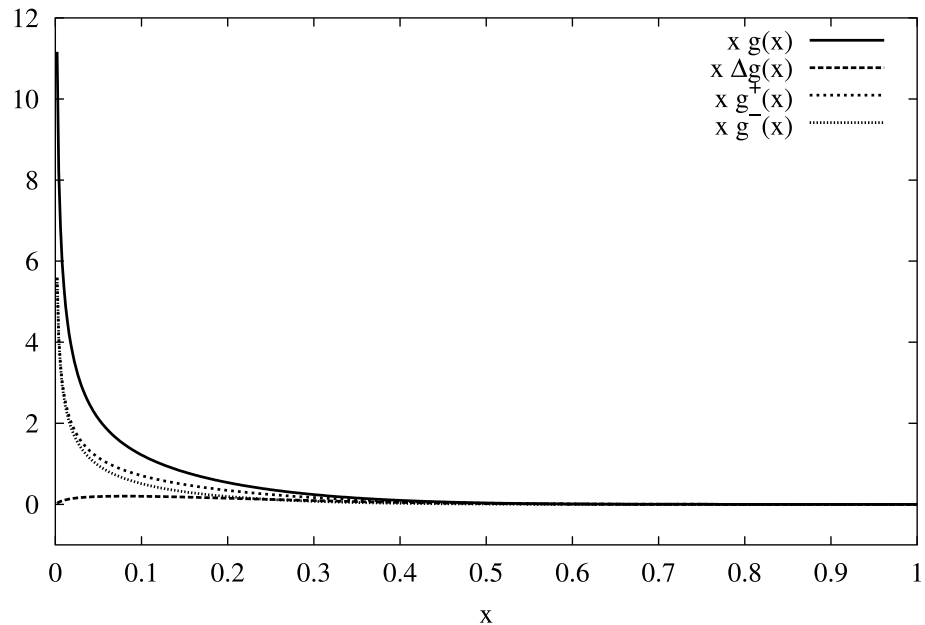


Figure 26: Various kinds of gluon distributions at $Q = 100$ GeV.

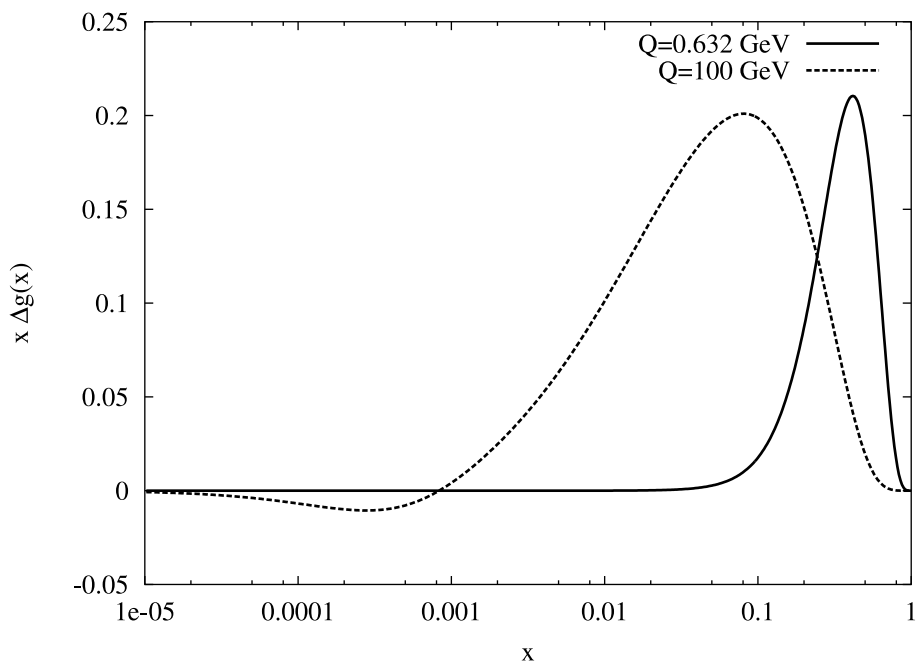


Figure 27: Small- x behaviour of Δg at 100 GeV.